Washington University School of Medicine
Digital Commons@Becker

Open Access Publications

2019

Repetitive concussive and subconcussive injury in a human tau mouse model results in chronic cognitive dysfunction and disruption of white matter tracts, but not tau pathology

Mihika Gangolli
Washington University in St. Louis

Joseph Benetatos
University of Queensland

Thomas J. Esparza
Washington University School of Medicine in St. Louis

Emeka M. Fountain
Washington University School of Medicine in St. Louis

Shamilka Seneviratne
Washington University School of Medicine in St. Louis

See next page for additional authors

Follow this and additional works at: https://digitalcommons.wustl.edu/open_access_pubs

Recommended Citation

Gangolli, Mihika; Benetatos, Joseph; Esparza, Thomas J.; Fountain, Emeka M.; Seneviratne, Shamilka; and Brody, David L., ,"Repetitive concussive and subconcussive injury in a human tau mouse model results in chronic cognitive dysfunction and disruption of white matter tracts, but not tau pathology." Journal of Neurotrauma.36,5. 735-755. (2019).
https://digitalcommons.wustl.edu/open_access_pubs/7705

This Open Access Publication is brought to you for free and open access by Digital Commons@Becker. It has been accepted for inclusion in Open Access Publications by an authorized administrator of Digital Commons@Becker. For more information, please contact engeszer@wustl.edu.

Authors
Mihika Gangolli, Joseph Benetatos, Thomas J. Esparza, Emeka M. Fountain, Shamilka Seneviratne, and David L. Brody

This open access publication is available at Digital Commons@Becker: https://digitalcommons.wustl.edu/open_access_pubs/7705

JOURNAL OF NEUROTRAUMA 36:735–755 (March 1, 2019)
© Mary Ann Liebert, Inc.
DOI: 10.1089/neu.2018.5700

Repetitive Concussive and Subconcussive Injury in a Human Tau Mouse Model Results in Chronic Cognitive Dysfunction and Disruption of White Matter Tracts, But Not Tau Pathology

Mihika Gangolli,[1] Joseph Benetatos,[2] Thomas J. Esparza,[3] Emeka M. Fountain,[3] Shamilka Seneviratne,[3] and David L. Brody[3]

Downloaded by Washington Univ from www.liebertpub.com at 05/06/19. For personal use only.

Abstract

Due to the unmet need for a means to study chronic traumatic encephalopathy (CTE) *in vivo*, there have been numerous efforts to develop an animal model of this progressive tauopathy. However, there is currently no consensus in the field on an injury model that consistently reproduces the neuropathological and behavioral features of CTE. We have implemented a repetitive Closed-Head Impact Model of Engineered Rotational Acceleration (CHIMERA) injury paradigm in human transgenic (hTau) mice. Animals were subjected to daily subconcussive or concussive injuries for 20 days and tested acutely, 3 months, and 12 months post-injury for deficits in social behavior, anxiety, spatial learning and memory, and depressive behavior. Animals also were assessed for chronic tau pathology, astrogliosis, and white matter degeneration. Repetitive concussive injury caused acute deficits in Morris water maze performance, including reduced swimming speed and increased distance to the platform during visible and hidden platform phases that persisted during the subacute and chronic time-points following injury. We found evidence of white matter disruption in animals injured with subconcussive and concussive injuries, with the most severe disruption occurring in the repetitive concussive injury group. Severity of white matter disruption in the corpus callosum was moderately correlated with swimming speed, while white matter disruption in the fimbria showed weak but significant correlation with worse performance during probe trial. There was no evidence of tau pathology or astrogliosis in sham or injured animals. In summary, we show that repetitive brain injury produces persistent behavioral abnormalities as late as 1 year post-injury that may be related to chronic white matter disruption, although the relationship with CTE remains to be determined.

Keywords: chronic behavior; concussive; subconcussive; white matter injury

Introduction

Chronic traumatic encephalopathy (CTE) is a progressive, neurodegenerative disease that cannot currently be diagnosed in living patients. Individuals with suspected CTE who are diagnosed postmortem typically have a history of repeated head impacts and often display mood and depressive type symptoms, typically manifesting approximately a decade following the initial impacts, followed by late stage cognitive failure.[1–3] The distinguishing neuropathological features of CTE, including depositions of phosphorylated tau (ptau) tangles and tau-positive astrocytes distributed in depths of cortical sulci and in perivascular regions, are initially observed in the superior and dorsofrontolateral prefrontal cortex. In later stages of CTE, neurofibrillary tangles and astroglial tau are found in the temporal lobe, hippocampus, amygdala, and inferior cortices.[4,5] Detection of these features is the only means to provide a diagnosis of CTE, and is performed using immunohistochemical staining of brain tissue. Therefore, an animal model of CTE would provide much needed insight, not only when developing diagnostic biomarkers, but also when testing potential therapeutics *in vivo*.

There have recently been numerous efforts to develop the necessary animal model of CTE using a variety of injury paradigms with mixed results (Supplementary Table 1; see online supplementary material at http://www.liebertpub.com). In wild-type mice, cognitive and social deficits, accompanied by depressive-like behavior manifest acutely following injury and are present as late as 6 months post-injury.[6–11] For example, Luo and colleagues implemented a repetitive closed head

[1]Department of Biomedical Engineering, [3]Department of Neurology, Washington University in St. Louis, St. Louis, Missouri.
[2]Queensland Brain Institute, University of Queensland, St. Lucia, Australia.

Downloaded by Washington Univ from www.liebertpub.com at 05/06/19. For personal use only.

impact model in adult mice that resulted in cognitive deficits during radial arm maze, increased ptau indicated by AT8 immunoreactivity, and astrogliosis indicated by glial fibrillary acidic protein (GFAP) immunoreactivity.[9] Concurrent work by Petraglia and colleagues used an increased number and frequency of impacts in adult mice that caused increased risk taking behavior and persistent Morris water maze deficits along with increased AT8 and GFAP immunoreactivity at both acute and chronic time-points.[7,8] In contrast, an early study by Yoshiyama and colleagues using transgenic mice overexpressing the shortest human isoform (T44) found no significant neurobehavioral differences or histopathological evidence of ptau tangles in injured animals 6 months following repeated injuries.[12] More recent work found that while repetitive closed headed impacts caused progressive behavioral impairments and neuroinflammation, there was no ptau pathology at chronic time-points up to 6 and 12 months post-injury using immunohistochemistry methods.[13,14] Further, studies of the temporal dynamics of ptau showed an acute increase followed by a return towards baseline at 30 days post-injury in wild-type mice, a finding paralleled in work by Yang and colleagues and Tran and colleagues using a single, more severe injury in triple transgenic 3xTG mice.[15–17]

The inconsistency of these initial findings raised the question of whether failures of previous attempts to reproduce the chronic and progressive ptau pathology seen in humans was due to the fundamental differences between tau in the human and mouse brain. While wild-type mice typically express only the 4R isoforms of tau, the human brain expresses 3R and 4R isoforms in equal amounts.[18–20] This furthers the motivation to study the chronic effects of repetitive traumatic brain injury in mice that express the tau isoforms seen in humans (hTau). These mice have been reported to develop age-associated thioflavin S neurofibrillary tangles between 9 and 15 months of age, along with cognitive deficits that manifest at 12 months of age.[18,21] Preliminary work exploring the relationship between brain injury and ptau pathology in the hTau mouse line was performed by Ojo and colleagues and showed that repetitive impacts in aged (18 months old) mice resulted in increased cortical ptau along with increased neuroinflammation.[22] The same group found that adult hTau mice exposed to repeated head injuries also had increased cognitive deficits along with elevated total tau levels at 6 months following injury.[23] These studies provide an initial insight into the role of repeated brain trauma and chronic ptau pathology but do not consistently show progressively worsening neurobehavioral deficits nor the neurofibrillary tangles and tau positive astrocytes that are pathognomonic for CTE.

Of note, all of the previously described models involved primarily impact injuries, whereas a large number of human concussive injuries appear most closely related to rotational acceleration.[24] Implementation of a rotational acceleration injury model in gyrencephalic animals such as pigs has resulted in accumulation of tau co-localized with beta-amyloid precursor protein (βAPP) and neurofilament staining indicative of axonal injury, illustrating the need to incorporate such a component in order to better mimic the brain trauma experienced during a concussive or subconcussive event.[25] The Closed-Head Impact Model of Engineered Rotational Acceleration (CHIMERA) is potentially advantageous for this very reason. This model combines high injury reproducibility with the ability to implement a nonsurgical impact plus rotational acceleration injury in small lower-cost animals, such as mice.[26] A recent study using three 0.5J injuries has resulted in chronic cognitive deficits accompanied by increased Iba1 and GFAP levels as late as 6 months post-injury.[27] Further, the versatility of impact thresholds at subconcussive and concussive levels has previously been tested and shows neurobehavioral and histopathological changes in the rodent brain.[28]

We have implemented a repetitive CHIMERA injury paradigm in hTau mice at two energy levels; concussive and subconcussive. The aim of the study is to determine the cumulative effects of repetitive brain trauma in adult mice (4 months of age) at acute (1 month), intermediate (3 months), and chronic (12 months) time-points post-injury. We hypothesized that the repeated impacts plus rotational acceleration would induce tissue shearing, white matter disruption, and in the chronic phase, accumulation of cortical and perivascular neurofibrillary tangles, astrogliosis, and white matter disruption accompanied by progressive neurobehavioral deficits comparable to those exhibited by patients with a diagnosis of CTE. As part of our pre-specified plan, cerebrospinal fluid (CSF) and blood was collected prior to sacrifice for exploration of potential fluid biomarkers of chronic phase repetitive concussive traumatic brain injury–related tau pathology.

Methods

Animals

Fifty hTau mice (C57BL/6 Cg-Mapt<tm1(EGFP)Klt>(MAPT), Cat #00549, Jackson Laboratory, Bar Harbor, ME) aged 4–8 weeks were purchased as two cohorts of 25 animals each. All mice were allowed to acclimate to 12-h light-dark cycles. Food and water were supplied *ad libitum.*

CHIMERA injury and anesthesia

Injuries were performed using the CHIMERA injury method, which involves a midline closed-head impact followed by rotational acceleration. Each animal was anesthetized with 5% isoflurane for 2.5 min followed by maintenance at 2.5% isoflurane during positioning on the platform. Total isoflurane exposure did not exceed 5 min and delivery was stopped immediately before impact. Sham animals underwent the same anesthesia protocol and head positioning on the CHIMERA device but no impact by the piston.

Determination of injury thresholds

Because animals were exposed to 20 daily impacts, the energy levels for subconcussive and concussive impacts were determined empirically (Supplementary Fig. 1A; see online supplementary material at http://www.liebertpub.com). Latency to right reflex (LRR), defined as the time from impact to regaining consciousness and becoming upright, was used as the acute metric of injury. In an initial study, wild-type mice (C57Bl6/J, Jackson Laboratory) were randomly assigned to receive a single impact with piston pressure set to range between 0 and 2.4 psi. Injuries were performed using the same anesthesia and head placement protocol described above, and righting time was recorded and used to determine the subconcussive threshold. Mice injured with piston pressures greater than 1.9 psi (0.13J energy intensity) all had mean righting times greater than the sham average.

Previous work using the CHIMERA device has determined that a single impact below 0.5J does not result in phenotypic deficits, including any increases in LRR time.[28] However, our pilot study with a single impact showed that animals receiving impacts between energy intensities of 0.13J and 0.24J (3.1 psi piston pressure) had increased LRR times (Supplementary Fig. 1A). Further, because we were interested in the cumulative effect of repeated injuries rather than a single impact, a second study was performed using wild-type mice. These mice were randomly assigned to receive $20\times$sham, 20×0.13J or 20×0.24J injuries spaced 24 ± 1 h apart. Righting times were recorded daily. The average righting time over the course of the 20 injuries was then calculated for each

group and analyzed using a one-way analysis of variance (ANOVA) followed by a *post hoc* Tukey's test (Supplementary Fig. 1B). There was a significant effect of injury in this study [$F(2,31) = 28.99$, $\eta^2_p = 0.652$, $p < 0.00001$]. Animals in the 0.24J group had increased righting times relative to shams and 20×0.13J mice (20×sham vs. 20×0.24J, $p = 0.000126$, 20×0.13J vs. 0.24J, $p = 0.000125$). Based on these data, we determined a subconcussive energy threshold of 0.13J and a concussive energy threshold of 0.24J.

Injury timeline

At 4 months of age, hTau mice were assigned to 20×concussive injury, 20×subconcussive injury, or 20×sham groups using a random number generator. Following impact or sham, each animal was placed supine in a warmed chamber (37°C) and monitored by an investigator blinded to injury status in a quiet, separate room until fully upright and ambulatory. LRR was recorded by this investigator. For sham animals, LRR was defined as the time from when isoflurane delivery was stopped to regaining consciousness. After regaining consciousness, each animal was returned to its home cage. This procedure was repeated for 20 consecutive days with injuries spaced 24 ± 1 h apart, such that each animal received 20 head impacts or sham procedures (Fig. 1A). A Cox regression for survival analysis was performed to determine the effect of injury on survival post-injury (Fig. 1B), and showed that there was a significant effect of injury status on survival ($p = 0.0304$), with a trend towards more deaths in the 20×concussive injury group.

Behavioral testing

All neurobehavioral testing was performed in a specified behavior room isolated from external noise and with light and sound controls. We controlled for 60 dB white noise (Marpac Dohm-DS, Wilmington, NC) and lighting (40 lux for Morris water maze, 20 lux for all other tests) for all testing. Neurobehavioral tests were performed during the work day (6 AM-6 PM). All equipment was cleaned with 70% ethanol prior to each test to remove scents. Animals were allowed to acclimate in the room for at least 1 h before testing. Following injuries, cages were renumbered such that the investigator remained blinded to injury status during the following behavioral testing. Behavioral testing was performed at three time-points: acutely, 3 months and one year following injuries. Acute behavioral testing began 22 days after the first injury (Fig. 1A). Social interaction testing was performed on Days 22–24, to provide sufficient testing time for each animal (25 min per animal with 5 min between animals). Acute elevated plus maze testing was performed 25 days after the first injury and acute open field testing was performed 28 days after the first injury. Acute Morris water maze testing began with the first day of the visible platform phase 29 days after the first injury and ending with the probe trial test 38 days after the first injury. Finally, acute tail suspension was performed 40 days after the first injury. Animals were allowed one day of rest between each test to minimize effects of stress induced by each behavioral assay. With the exception of tail suspension, all tests were recorded on video and subsequently analyzed using Panlab SMART (Harvard Bioscience, Holliston, MA).

Social interaction and social novelty. Crawley's three-chamber test was used to measure social interaction and social novelty.[29] Test mice were singly housed for 24 h prior to testing. On testing day, the test mouse was placed in a 42×70 cm three-chamber box made of opaque white plastic. Following a 5 min habituation session where the mouse was allowed to freely explore all three chambers, the test mouse was then confined to the middle chamber during preparation for the preference for sociability session. A stimulus mouse (male C57BL/6 aged 6–8 weeks) was placed in a wire cage in one chamber while a dummy mouse made of black Legos was placed in a wire cage in the opposite chamber. The test mouse was then allowed to explore all three chambers for 10 min. The test mouse was then confined again to the middle chamber prior to preference for social novelty testing. The dummy mouse used

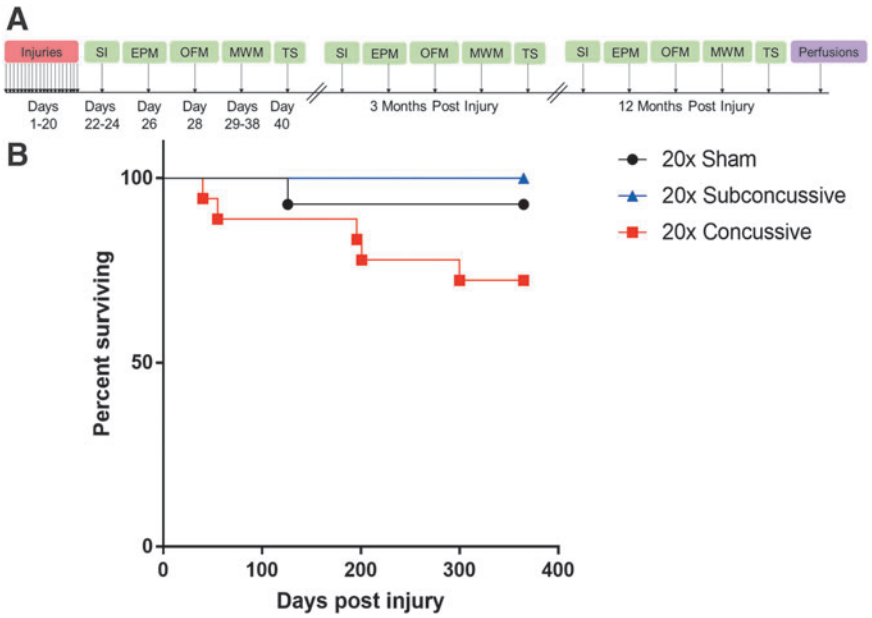

FIG. 1. Injury timeline and survival post-injury. **(A)** Fifty male hTau mice were purchased in two separate cohorts. Animals were randomly assigned to sham, 20×subconcussive (0.13J) or 20×concussive (0.24J) injury groups. Following 20 days of injuries, behavioral outcomes including social interaction (SI), elevated plus maze (EPM), open field maze (OFM), Morris water maze (MWM) and tail suspension (TS) were assessed acutely, at 3 months, and 1 year post-injury. Following the 12-month behavioral test session, all animals were perfused. **(B)** Survival and mortality risk were assessed using a Cox survival and hazard regression analysis. The data showed a modest but significant ($p = 0.03$) effect of subconcussive or concussive injury on mortality rate. Color image is available online.

Downloaded by Washington Univ from www.liebertpub.com at 05/06/19. For personal use only.

during sociability testing was replaced with a novel stimulus mouse (male C57BL/6 age 6–8 weeks). The test mouse was then allowed to explore all three chambers for 10 min. Because each testing session required approximately 30 min of test time, stimulus mice were used in pairs and allowed to rest while a second pair of stimulus mice was used for the next test mouse. Time spent interacting with each mouse was measured by tracking the time the mouse spent sniffing within a 1.5 cm radius around each wire cage. Activity such as climbing on top of the wire cage was not counted as interaction.

Elevated plus maze. A custom maze (30 cm high) with arms that were 30 cm long and 5 cm wide was used for testing. Closed arms were enclosed by 16 cm high walls while open arms had a 2-mm railing to prevent mice from falling. Mice were placed in a closed arm and allowed to explore the maze for 5 min. A 5 cm square was defined as the center zone, requiring the mouse to have all four paws in an arm of the maze to be quantified in SMART as being in that arm. Time spent in all zones (open arms, closed arms, center zone) was quantified using SMART.

Open field test. Mice were placed in a 44.5×44.5 cm box made of white opaque plastic and allowed to explore for 5 min. Thigmotactic behavior was defined as the average distance away from the wall. Briefly, the time spent moving was measured using Panlab SMART. During video analysis the box was divided into 15 concentric zones spaced 1.5 cm apart. Time spent in each zone was weighted by zone distance from the maze wall and summed to obtain a time-weighted average.

Morris water maze. A 120 cm diameter pool was filled with 22°C water made opaque using non-toxic white tempera paint. For each day except for probe trial, mice were required to swim for four trials per day, and were inserted into four locations in the pool (NW, SW, SE, NE) and allowed to swim for a maximum of 1 min to reach the 11 cm platform. The order of insertion points was changed each day. During the visible platform phase (3 days, Wednesday-Friday), a flag was placed on the platform so that it would be clearly visible. For the hidden platform phase (4 days, Monday-Thursday), opaque white curtains were hung to enclose the pool, with prominent visual cues in each quadrant. The platform was then moved to a different quadrant and the water level was increased so that the platform was hidden under 1 cm of opaque white water. To control for memory retention between test sessions, the hidden platform was placed in a different quadrant for each test session. For hidden and visible platform testing, the average distance swum, average swim speed, and latency to platform were recorded and calculated using Panlab SMART. Twenty-four hours following the final day of hidden platform testing, the platform was removed from the pool. Mice were then subjected to a single probe trial, where each mouse was inserted at the insertion point furthest from where the hidden platform had previously been and allowed to swim for 30 sec. The percentage of time spent in the target quadrant, as well as mean proximity from the platform, were recorded and calculated using Panlab SMART.

Tail suspension. A white paper cone was placed on each animal's tail to prevent climbing behavior commonly exhibited in C57Bl/6 mice. Mice were then suspended from a rod at a height of 30 cm by their tails. The total test time was 6 min. Time immobile, defined as any time the mouse was not moving except swinging from previous movement, was recorded manually by an investigator blinded to injury status.

CSF, blood, and tissue collection

Following the 1-year time-point of behavioral testing, mice were sacrificed. Animals were randomly assigned a new identification number to assure blinding during histological analysis. Mice were anesthetized with a 75 mg/kg dose of pentobarbital administered IP. When mice remained unresponsive to tail or toe pinch, they were placed on a pad heated to 37°C, and CSF was extracted from the cisterna magna.[30] Mice were then transcardially perfused using ice cold 0.3% phosphate-buffered saline (PBS)-heparin solution and approximately 800 μL of blood was collected using the cardiac bleeding method. Following tissue extraction, the brain was separated into two hemispheres. The left hemisphere was drop fixed overnight in 4% paraformaldehyde and then switched to 30% sucrose solution, stored at 4°C. The right hemisphere was dissected on a chilled aluminum foil plate into cortical and hippocampal regions and stored at −80°C. Blood samples were allowed to clot for a minimum of 1 h, and then blood and CSF were centrifuged at $2000 \times g$ to extract serum samples, which were stored at −80°C. Results from CSF, blood and frozen brain tissue analyses will be reported separately.

Immunohistochemistry

Fixed brain tissue was sectioned coronally into 50-μm thick sections using a freezing sliding microtome (Microm HM 430, ThermoFisher Scientific, Waltham, MA) in a 1:6 series and stored in cryoprotectant (sucrose dissolved in sodium phosphate buffer, pH 7.4 and ethylene glycol) at 4°C. Total human tau was detected using monoclonal HT7 (Cat# MN1000, ThermoFisher Scientific). Primary antibodies used to detect phosphorylated tau included monoclonal AT8 (Cat# MN1020, ThermoFisher Scientific), CP13 (courtesy of Peter Davies, Albert Einstein College of Medicine, NY) and RZ3 (courtesy of Peter Davies). Astrocytes and activated microglia were detected with polyclonal GFAP (Cat# AB5541, Millipore Sigma, St Louis, MO) and polyclonal Iba1 (Cat# 019-19741, Wako Chemicals USA Inc., Richmond, VA) respectively. APP immunoreactivity was detected using polyclonal βAPP (Cat# 51-2700 Invitrogen, Camarillo, CA). For tau staining, antigen retrieval was performed using a 5-min incubation in 70% formic acid. Sections were then incubated in 0.3% hydrogen peroxide solution to block endogenous peroxidase and then blocked for 30 min in 3% serum diluted in TBS-X. Normal goat serum (Cat# S-1000, Vector Laboratories, Burlingame, CA) was used for tau, Iba1 and APP staining, while normal donkey serum (Cat# 017-000-121, Jackson Immunoresearch, West Grove, PA) was used for GFAP staining. Sections were then incubated overnight at 4°C in primary antibody diluted 1:1000 in 3% serum. Tissue from an uninjured 22-month-old 3xTG mouse was used as a positive control for tau pathology, while tissue from a mouse injured using the controlled cortical impact injury model was used as a positive control for GFAP, Iba1 and APP staining.[31,32] Negative controls with the primary antibody excluded were performed for all stains. The next day, sections were incubated in secondary antibody diluted 1:1000 in TBS-X for 1 h. For tau staining, biotinylated goat anti-mouse secondary antibody (Cat# BA-9200, Vector Laboratories) was used while biotinylated donkey anti-chicken secondary antibody (Cat# 703-065-115, Jackson Immunoresearch) was used for GFAP staining. Biotinylated goat anti-rabbit secondary antibody (Cat# BA-1000, Vector Laboratories) was used for Iba1 and APP staining Sections were incubated for one 1 h in ABC solution (Cat# PK-6100, Vector Laboratories) diluted 1:400 A and B in 1xTBS, followed by visualization using 3′3′ diaminobenzidine (Cat# D5905-100TAB, Sigma Aldrich, St. Louis, MO). Sections were washed three times in $1 \times$TBS between each step.

Myelin Black Gold II staining

Tissue sections were first washed in TBS to remove residual cryoprotectant. Black Gold II solution was prepared by resuspending 150 mg dry Black Gold II powder (Cat# AG400, Millipore Sigma) in 0.9% saline solution. The Black Gold II solution

Downloaded by Washington Univ from www.liebertpub.com at 05/06/19. For personal use only.

Downloaded by Washington Univ from www.liebertpub.com at 05/06/19. For personal use only.

was then heated to 60°C. Free-floating tissue sections were incubated in the solution for 8–12 min until fibers were completely stained (Supplementary Fig. 2; see online supplementary material at http://www.liebertpub.com). Following two washes in Milli-Q water, sections were incubated in 0.1% sodium thiosulfate solution heated to 60°C for 3 min. The tissue sections were then washed three times in TBS to remove trace sodium thiosulfate.

Quantification of histology

Following staining, tissue sections were mounted onto positively charged slides, dehydrated in a series of graded ethanols (50%-70%-95%-100%-100%), and cleared in three changes of xylenes before being cover-slipped (No. 1.5, Cat # 48393-241; VWR). Images of stained sections were acquired on a Zeiss Axioscan (Carl Zeiss AG, Oberkochen, Germany) using a brightfield 10× objective lens and then exported at their original resolution into tiff format for quantification. Regions of interest (ROIs) in the gray matter included cortical gray matter (4–5 sections/animal), lateral septal nucleus (1 section/animal), and the hippocampus (3–4 sections/animal). White matter intact (> 50% of region without folds or tears) ROIs included the corpus callosum (4–5 sections/animal) anterior commissure (one section/animal), hippocampal commissure (1 section/animal) and fimbria (2 sections/animal).

To quantify GFAP staining, the Renyi entropy thresholding method was applied to all images (Supplementary Fig. 3; see online supplementary material at http://www.liebertpub.com). The Sauvola local thresholding method (radius of 15) was used to quantify microglial cell bodies stained using Iba1. Similar to Myelin Black Gold II analysis, ROIs were included and considered intact only if >50% of the region was without folds or tears. To exclude remaining edge and fold artifacts, only particles with an area of 10–500 pixels were included in analysis.

Because there were no signs of severe demyelination in any of the tissue sections, we used power coherence as a measure of white matter integrity as previously described.[33] Briefly, each ROI was subdivided into square regions with an area of 10 pixels^2. This area was used to sustain sufficient spatial resolution and prevent artifacts caused by multiple crossing fibers, while also removing noise related artifacts. A two-tensor model was then fit to the power spectrum of each subdivided region. Power coherence, a metric ranging from 0 to 1, was calculated by subtracting the ratio of the major and minor axes of the tensors from one.

PCR confirmation of genotype

PCR was used to confirm the hTau genotype from one animal selected at random from each cohort of hTau mice. DNA from the leftover regions of the fresh-frozen brain tissue was extracted using the EZ High MW Mouse Tail DNA Isolation Kit (Cat# M1007-100, EZ Bioresearch, St. Louis, MO). Nuclei lysis and Proteinase K solution were added to the tissue sample and incubated overnight at 55°C with gentle shaking until the tissue was completely digested. The next day, protein precipitation solution was added to the mixture. Following a 5-min incubation on ice, the solution was centrifuged at 16,000× g for 3 min at room temperature, separating the protein pellet from supernatant. Isopropanol was added to the supernatant and inverted until DNA was visible as threads. The supernatant and isopropanol solution was then centrifuged 16,000× g for 1 min at room temperature. The supernatant was then removed from the microcentrifuge tube and the remaining DNA pellet was washed with 70% ethanol. The DNA pellet was centrifuged and washed again with 70% ethanol. Any residual supernatant was then removed and the DNA pellet was allowed to air dry for 10 min. DNA Hydration Solution was added to the pellet and incubated at 65°C for 1 h with gentle shaking. The extracted DNA was then stored at 4°C until PCR genotyping. Tail DNA from an hTau mouse was obtained from an independent investigator to use as an external positive control.

Control (hTau ctrl R : 5′- GTA GGT GGA AAT TCT AGC ATC ATC C -3′, hTau ctrl F : 5′- CTA GGC CAC AGA ATT GAA AGA TCT -3′) and hTau specific oligonucleotides (hTau R : 5′- CTC TGC ATG GCT GTC CAC TAA CCT T -3′, hTau F : 5′- ACT TTG AAC CAG GAT GGC TGA GCC C -3′) were resuspended to 100 μM concentration in molecular grade water. The extracted DNA was thawed on ice and diluted to a final concentration of 100 ng/μL. A solution of DNA, control or hTau oligonucleotides (0.2 μM), GoTaq Flex (Promega, Madison, WI), deoxyribonucleotide triphosphates, reaction buffer, and enhancer was then prepared in molecular grade water and heated using a thermocycler. Thermocycler conditions were 94°C for 30 sec, 58°C for 1 min, and 72°C for 1 min for 35 cycles each, with a final extension phase of 72°C for 2 min. PCR was visualized on a 1% agarose gel.

Western blotting

Western blotting for total human tau and phosphorylated tau was performed as previously described.[17,34] Briefly, frozen hippocampi from 5–6 randomly selected animals from each injury group were homogenized in RIPA buffer with added protease and phosphatase inhibitors. Hippocampal tissue from an uninjured 22-month-old 3xTG animal was used as a positive control for total and phosphorylated tau. Homogenates were centrifuged (13,000 rpm, 20 min at 4°C) and protein concentrations were determined using the bicinchoninic acid assay methods in order to obtain equal amounts of protein sample. Samples were then heated with mercapto-ethanol. Dot blot analysis was performed by pipetting 100 μg of protein onto 0.2 μm nitrocellulose membranes which were then allowed to dry completely. In parallel, 20 μg of protein with loading buffer was loaded per well and then electrophoresed on 10% BisTris NUPAGE gels (Cat#NP0301, ThermoFisher Scientific, Carlsbad, CA), followed by transfer to 0.2 μm nitrocellulose membranes. These membranes were blocked with 5% milk in PBS with Tween (PBS-T) for 1 h, followed by incubation in primary antibody (HT7, total human tau or AT8, ptau) diluted 1:1000 in 5% milk in TBS-T overnight at 4°C. Antibodies were detected using sheep anti-mouse horseradish peroxidase (GE Healthcare, Cat#NXA931, Buckinghamshire, UK; 1:10,000 dilution in 5% milk and PBS-T solution) and ECL Western blotting kit (GE Healthcare, Cat#RPN2235, Buckinghamshire, UK). Membranes were then stripped and reprobed for tubulin (1:1000 dilution).

Statistical analysis

All analysis was performed using Statistica (Tibco Software Inc., Palo Alto, CA). All data was tested for normality using the Shapiro-Wilk normality test. Any datasets that violated the assumption of normality were transformed so that parametric analyses could be performed (Supplementary Table 2; see online supplementary material at http://www.liebertpub.com). A two-way, repeated measures ANOVA was performed for each neurobehavioral metric to test for the effects of injury and cohort, with test session (acute, 3-month, one1data and histological data. We pre-specified the statistical plan to collapse across the two cohorts of mice for analyses for which there were no significant main effects or cohort of interactions with of other factors with cohort. Statistical power calculations for main effects of injury was 80% at $p < 0.05$ with an effect size of 0.50. Animals that died before the end of the experiment were excluded from behavioral and histological analysis. *Post hoc* Tukey's tests were then used to determine significance for specific pairwise comparisons ($p < 0.05$). Because the residuals were not normally distributed, all correlational analyses were performed using Spearman's rank correlations, followed by Bonferroni correction for multiple comparisons. The relationship between power coherence and microgliosis in white matter tracts was assessed using Spearman's correlations, followed by Bonferroni correction for multiple comparisons. When determining the relationship between white matter power coherence and Morris

water maze measures (four ROIs × five behavioral measures = 20 correlations), the effective number of tests was adjusted to account for potential correlation between measures.[35] Without this adjustment, the Bonferroni correction at $p < 0.05/20 = 0.0025$; however, with the variance of the eigenvalues of the correlation matrix ($v\lambda obs = 1.265$), the adjusted Bonferroni at $p < 0.05/18.79 = 0.0027$.

Correlations between microgliosis in both gray and white matter with Morris water maze measures (seven ROIs × five behavioral measures = 35 correlations) were similarly adjusted. After adjustment using the variance of the eigenvalues of the correlation matrix ($v\lambda obs = 1.041$), the adjusted Bonferroni at $p < 0.05/33.99 = 0.0015$. Effect sizes were calculated for each test that was performed (Supplementary Table 3; see online supplementary material at http://www.liebertpub.com). Graphs were plotted using Prism v7.0 (Graph Pad, La Jolla, CA). All error bars represent standard error of mean (SEM).

Results

hTau mice show injury dependent differences in righting time

Loss of consciousness, measured by righting time (LRR) was used to measure the immediate effects of injury during the 20 days of impacts (Fig. 2). LRR was calculated by measuring the righting time each day of injury, and averaging across days. A two-way ANOVA showed that there was a significant effect of injury [$F(2,44) = 11.8092$, $\eta^2_p = 0.349$, $p < 0.0001$]. Animals in the 20× concussive group had elevated righting times compared with 20× shams ($p = 0.00059$); as well as animals in the 20× subconcussive group ($p = 0.00046$) after *post hoc* Tukey's testing. There was no difference in righting times between 20× shams and animals in the 20× subconcussive group ($p = 0.985$). There was no effect of cohort or interaction between injury and cohort. These data show that the higher-energy concussive impacts caused a significantly more substantial acute injury than the lower-energy subconcussive impacts.

hTau mice subjected to repeated concussive injuries show persistent chronic cognitive deficits

At acute, 3-month and 12-month time-points, animals were tested for learning deficits using the Morris water maze task. During the 3 days of visible platform testing (Fig. 3; Supplementary Fig. 4; see online supplementary material at http://www.liebertpub.com), the two-way, repeated measures ANOVA, showed a main effect of injury on swim speed [$F(2,36) = 29.9335$, $\eta^2_p = 0.624$, $p < 0.00001$]. Animals in the 20× concussive group had reduced swim speeds relative to both shams ($p = 0.000127$) and mice in the 20× subconcussive injury group ($p = 0.000128$). There was no interaction between test session (acute, 3-month, 12 month) and injury. There was also a main effect of injury on distance to the target [$F(2,36) = 25.642$, $\eta^2_p = 0.588$, $p < 0.00001$]. Animals in the 20× concussive group had increased swimming distances relative to shams ($p = 0.000127$) and mice in the 20× subconcussive injury group ($p = 0.000127$). There were no differences between subconcussive injury and sham groups ($p = 0.923$). There was no effect of test session or interaction between test session and injury on swim speed or distance swum.

At each test session, 2 days following the final day of visible platform testing, animals underwent hidden platform testing of the Morris water maze task for 4 consecutive days (Fig. 4; Supplementary Fig. 5; see online supplementary material at http://www.liebertpub.com). Similar to the visible platform phase, the two-way repeated measures ANOVA showed an effect of injury on swim speed [$F(2,36) = 36.5009$, $\eta^2_p = 0.663$, $p < 0.00001$] that remained significant after *post hoc* testing. Mice in the 20× concussive group had reduced swim speeds relative to 20× shams ($p = 0.000125$) and mice in the 20× subconcussive group ($p = 0.000128$). Animals in the 20× subconcussive group also had reduced swimming speeds relative to 20× shams ($p = 0.028$). There also was an effect of injury on swimming distance during the hidden platform phase [$F(2,36) = 6.272$, $\eta^2_p = 0.564$, $p < 0.01$] that remained significant following *post hoc* Tukey's testing. Animals in the 20× concussive group had increased swimming distances relative to 20× shams ($p = 0.044$) and animals in the 20× subconcussive group ($p = 0.009$). There was no difference in swimming distance between subconcussive injury and sham groups ($p = 0.867$). There no effect of test session on either swim speed or swimming distance. There was also was no interaction between test session and injury on either of these measures.

Twenty-four hours after the final day of hidden platform testing, hTau mice were tested for memory retention using the probe trial of the Morris water maze task (Fig. 5; Supplementary Fig. 6; see online supplementary material at http://www.liebertpub.com). Mean proximity to platform and percent time spent in the target quadrant were used as metrics of memory retention for each test session. For the measure of mean proximity to platform, there was an effect of injury [$F(2,36) = 23.173$, $\eta^2_p = 0.570$, $p < 0.00001$] and time [$F(2,70) = 6.9935$, $\eta^2_p = 0.167$, $p < 0.01$] on mean proximity to platform that remained significant after *post hoc* testing. Animals in the 20× concussive injury group were further away from where the hidden platform had previously been placed relative to both shams

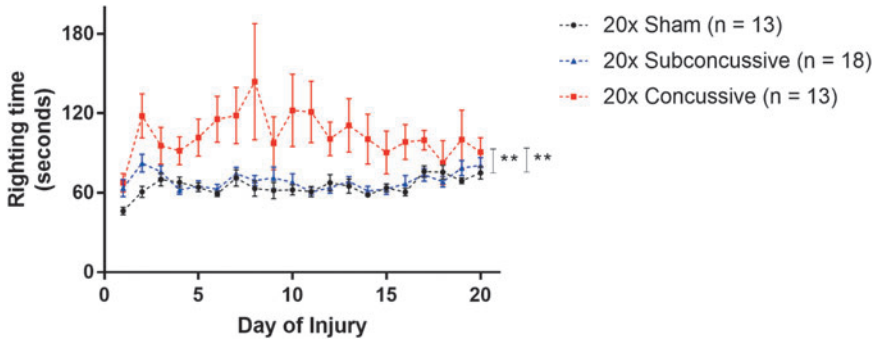

FIG. 2. Loss of consciousness following injury. Latency righting reflex was used as a measure loss of consciousness. Righting times were measured by an observer blinded to injury status. Animals in the concussive injury group had increased righting times relative to the subconcussive and sham groups, which were indistinguishable. There was a significant effect of concussive injury on righting time, with animals in the 20× concussive group having increased righting times relative to 20× shams ($p = 0.00059$) and 20× subconcussive mice ($p = 0.00046$). Color image is available online.

Downloaded by Washington Univ from www.liebertpub.com at 05/06/19. For personal use only.

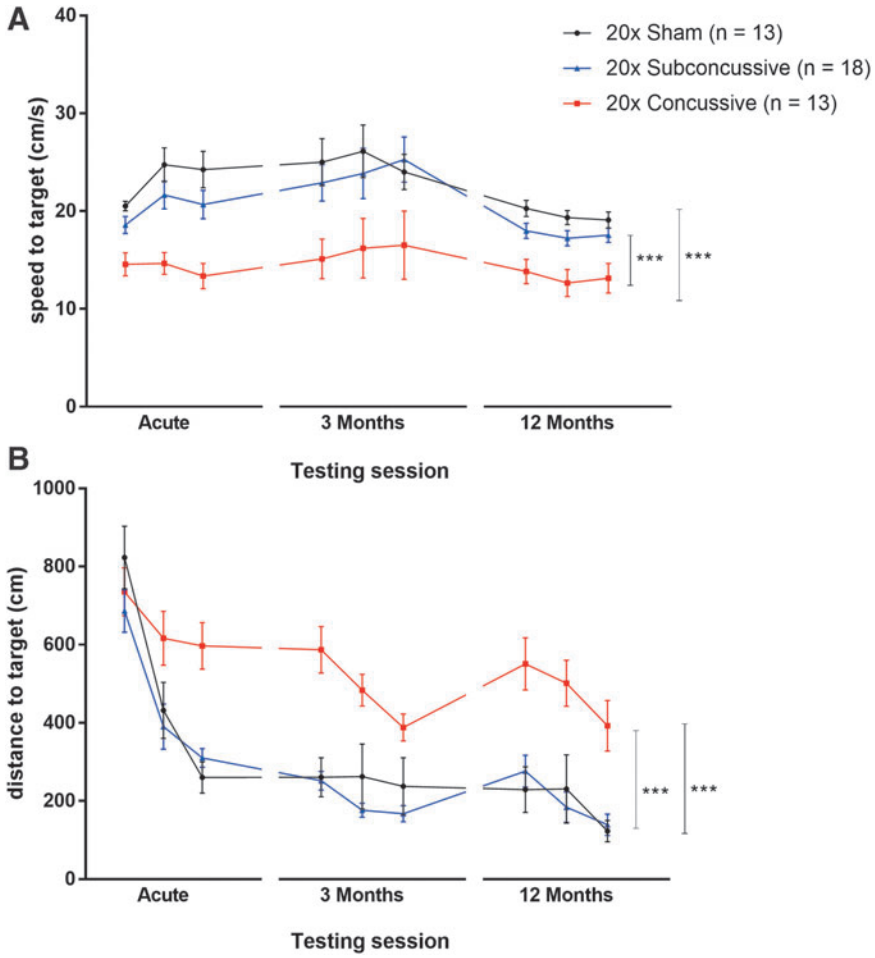

FIG. 3. Effects of injury on visible platform phase of the Morris water maze. **(A)** Average swimming speeds for each day of the visible phase of the Morris water maze during each of the three test sessions. There was a significant effect of injury on swim speed (0.24J vs. sham: $p = 0.000127$, 20× concussive vs. 20× subconcussive; $p = 0.000128$). There was no interaction between test session and injury. **(B)** Total distance to the target platform during 3 days of visible platform testing. There was a significant effect of repetitive concussive injury (20× concussive vs. sham: $p = 0.000127$, 20× concussive vs. 20× subconcussive: $p = 0.000127$). Color image is available online.

($p = 0.000124$) and 20× subconcussive animals ($p = 0.000126$). Animals also had increased proximity to the target platform during the 3-month test session ($p = 0.000280$) relative to the acute test session. There was also an effect of injury on percent time in the target quadrant [$F(2,36) = 22.851$, $\eta^2_p = 0.566$, $p < 0.00001$] that remained significant after *post hoc* testing. These same animals also spent significantly less time in the target quadrant relative to shams ($p = 0.000124$) and 20× subconcussive animals ($p = 0.000123$). There were no significant differences between animals in the 20× subconcussive group or 20× sham group for either proximity to platform or percent time spent in the target quadrant. There was no interaction between time and injury for either parameter.

In summary, repetitive concussive injury resulted in reduced swim speed during both visible and hidden platform phases of Morris water maze, a possible indication of reduced motor function or motivation following injury. Further, repetitive concussive injury also caused an increase in distance swum to the target. This effect indicates an impairment in ability to learn the platform location. Moreover, repetitive concussive injury resulted in impaired memory, demonstrated by increased proximity to platform and reduced percent time in target quadrant during the probe trial. These findings, combined with the effect of time on proximity to the platform during only intermediate session of probe trial indicates that the 20× concussive injury method implemented in this study causes acute cognitive deficits that neither progressively worsen nor resolve at 1 year post-injury. Instead, these changes in learning and memory appear to remain sustained at a reduced level relative to shams and animals in the 20× subconcussive group.

No social interaction deficits, anxiety or depressive-like behaviors detected after repeated injury in hTau mice

The sociability and social novelty phases of Crawley's three-chamber social interaction test were used to measure both acute and chronic social behaviors (Fig. 6; Supplementary Fig. 7; see online supplementary material at http://www.liebertpub.com). For the sociability test, the ratio of time spent interacting with the stimulus mouse to time spent interacting with the novel object was used as an index of sociability. For the social novelty test, the ratio of time spent interacting with the novel mouse to time spent interacting with the previous stimulus mouse was used as an index of social novelty. The two-way repeated measures ANOVA showed no effect of injury on either sociability index [$F(2,37) = 0.300$, $p = 0.74$] or social novelty testing index [$F(2,37) = 2.729$, $p = 0.78$]. There also was no effect of test session on either index.

Downloaded by Washington Univ from www.liebertpub.com at 05/06/19. For personal use only.

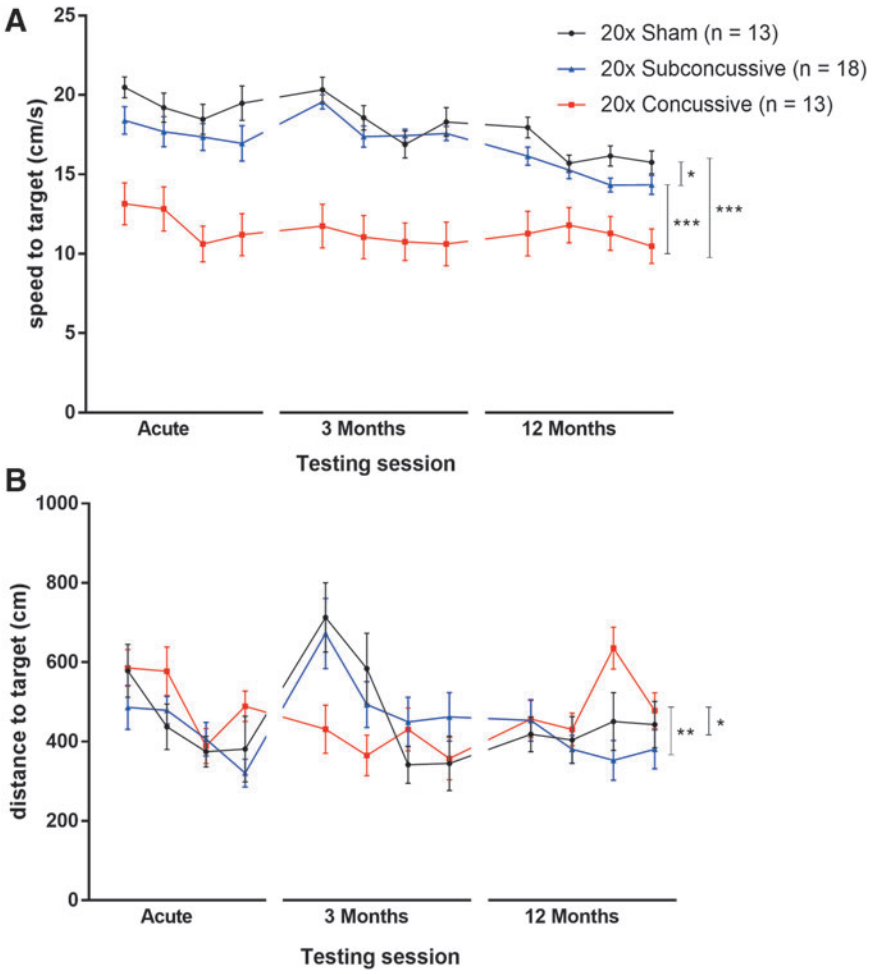

FIG. 4. Effects of injury on hidden platform phase of the Morris water maze. **(A)** Average swimming speeds for each of the 4 days of the hidden platform task during each of the three test sessions. There was a significant effect of injury (20×concussive vs. sham, $p=0.000125$, 20×concussive vs. subconcussive, $p=0.000128$). Mice in the 20×subconcussive group also had reduced swimming speeds relative to shams ($p=0.028$). **(B)** Total distance to the target platform during four days of hidden platform testing. There was a significant effect of concussive injury (20×concussive vs. sham: $p=0.044$, 20×concussive vs. 20×subconcussive: $p=0.009$). There was no interaction of test session and injury. Color image is available online.

Downloaded by Washington Univ from www.liebertpub.com at 05/06/19. For personal use only.

Anxiety-like behavior was measured using two behavioral measures: open arm time during the elevated plus maze task, and thigmotaxis during the open field maze task (Fig. 7; Supplementary Fig. 8; see online supplementary material at http://www.liebertpub.com). Animals displaying increased risk taking and anxious behavior would be expected to have increased open arm time and elevated thigmotaxis scores. There was no effect of injury on open arm time [$F(2,37)=0.195$, $p=0.98$]. While the two-way repeated measures ANOVA did show an effect of injury on open field thigmotaxis [$F(2,37)=3.610$, $p=0.0367$] there were no significant differences between groups following *post hoc* testing. There was no effect of test session on open arm time or thigmotaxis.

Time immobile during the tail suspension test was used as a metric of depressive-like behavior (Fig. 8; Supplementary Fig. 9; see online supplementary material at http://www.liebertpub.com). The two-way repeated measures ANOVA showed an effect of injury on immobility time [$F(2,37)=12.954$, $p<0.0001$] that remained significant after *post hoc* testing. hTau mice in the 20×concussion group showed reduced immobility times rather than the expected increased immobility times relative to shams ($p=0.00427$) and relative to mice in the subconcussive group ($p=0.000212$). The interpretation of this result is not clear (see Discussion). There was no significant difference between animals in the 20×subconcussive group and 20×shams ($p=0.546$). There also was no significant effect of test session on time spent immobile, though it appeared that the effect was less apparent at the 3-month test session. These findings show that repetitive concussive or subconcussive injury does not result in acute social, anxiety related, or depressive-like deficits. Further, based on the lack of an effect of test session, deficits in these domains do not manifest during the chronic stages following injury.

Repetitive brain injury does not result in chronic astrogliosis

GFAP staining was used to assess the effect of repetitive head injury on chronic astrogliosis. Regions of interest were drawn in the gray matter (cortex, lateral septal nucleus and hippocampus) and white matter (corpus callosum, anterior commissure, hippocampal commissure and fimbria). Percent area of positive staining was used as a measure of astrogliosis. The two-way ANOVA showed no effect

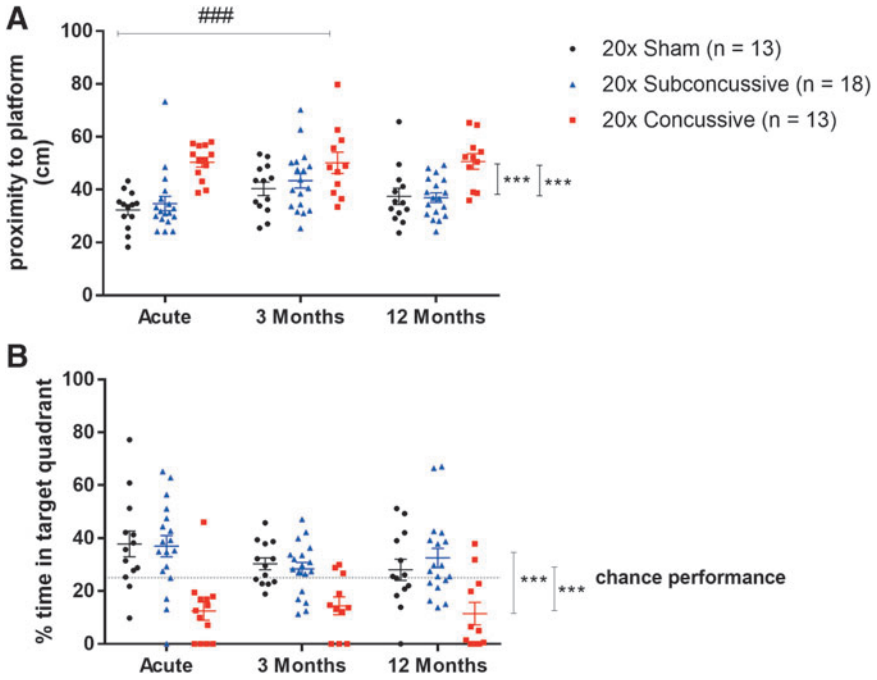

FIG. 5. Effects of injury on Morris water maze probe trial performance. **(A)** There was a significant effect of concussive injury on average proximity to platform during probe trial; 20×concussive vs. 20×sham: $p=0.000124$, 20×concussive vs. 20×subconcussive: $p=0.000126$). There was also an effect of time, where animals were significantly further away from the platform at the 3-month test session ($p=0.000280$) relative to the acute session (###). Animals in the repetitive concussive injury group were on average further away from the location of the target platform. **(B)** There was a significant effect of concussive injury on the percent time spent in the quadrant where the platform had previously been placed (20×concussive vs. sham: $p=0.000124$, 20×concussive vs. 20×subconcussive: $p=0.000123$). Animals in the repetitive concussive injury group tended to spend less than 25% of their time (chance performance, dotted line) in the target quadrant. There was no interaction between test session and injury. Color image is available online.

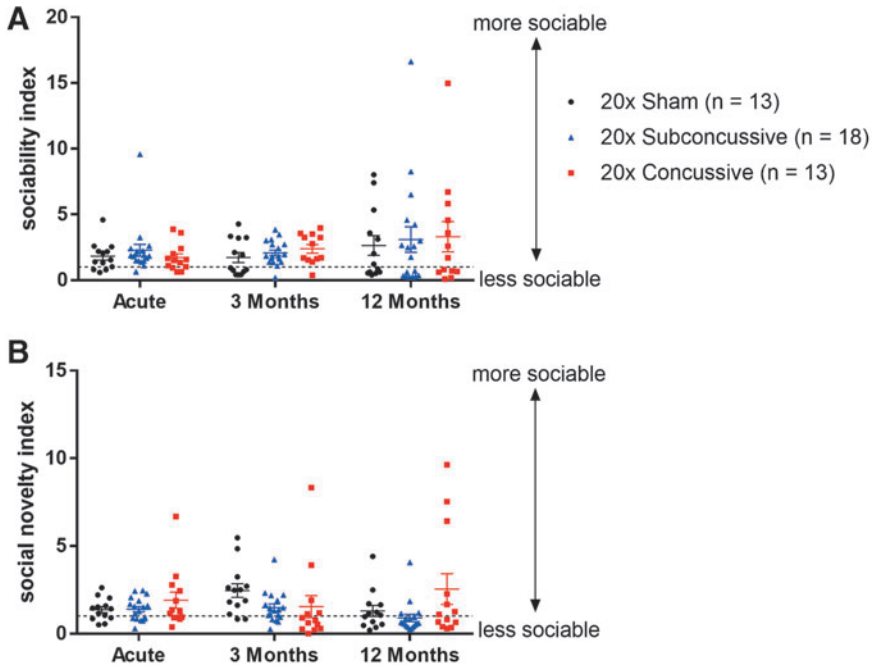

FIG. 6. No change in social interaction following injury. **(A)** Injured animals did not show any significant changes in sociability compared with shams. Dotted line indicates a sociability index of 1. Points above this line indicate that the animal showed preference for the stimulus mouse rather than the novel inanimate object. **(B)** Injured animals did not show any significant changes in social novelty compared with shams. Dotted line indicates a social novelty index of 1. Points above this line indicate that the animal showed preference for the novel mouse rather than the stimulus mouse from the previous sociability session. Color image is available online.

Downloaded by Washington Univ from www.liebertpub.com at 05/06/19. For personal use only.

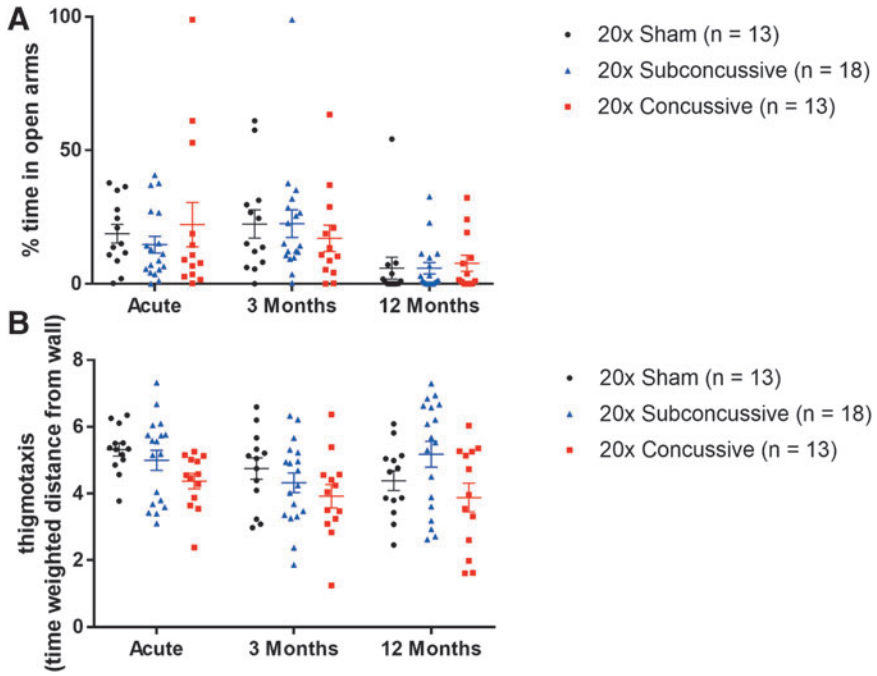

FIG. 7. No changes in anxiety related behavior following injury. **(A)** Animals in the 20×concussive and 20×subconcussive did not show any changes in percent time spent in open arms of the elevated plus maze relative to shams. **(B)** Injured animals did not show any changes in open field thigmotaxis (time weighted distance from the wall) relative to sham animals. Color image is available online.

of injury ($p > 0.05$ all regions; details in Supplementary Table 3) on percent area of GFAP staining in any of the regions of interest (Fig. 9). In summary, our analysis of activated astrocytes shows that our 20×concussion model does not result in chronic astrogliosis.

Repetitive brain injury results in chronic microgliosis in the corpus callosum

Iba1 staining was used to determine whether there was an effect of repetitive head injury on chronic microgliosis. Regions of interest were drawn in the gray matter (cortex, lateral septal nucleus and hippocampus) and white matter (corpus callosum, anterior commissure, hippocampal commissure and fimbria). Percent area of positive thresholded staining was used to quantify the extent of microgliosis in each region. For all regions except for the corpus callosum, the two-way ANOVA showed no effect of injury (Supplementary Fig. 10, $p > 0.05$; see online supplementary material at http://www.liebertpub.com; details in Supplementary Table 3). In the corpus callosum, the two-way ANOVA revealed that there was an effect of injury on microgliosis [$F(2,34) = 7.984$, $\eta^2_p = 0.320$, $p < 0.01$]. *Post hoc* Tukey's testing showed that animals in the repetitive concussive injury group had modest increases in microgliosis in the corpus callosum (Fig. 10; $p = 0.0327$). These findings show that repetitive

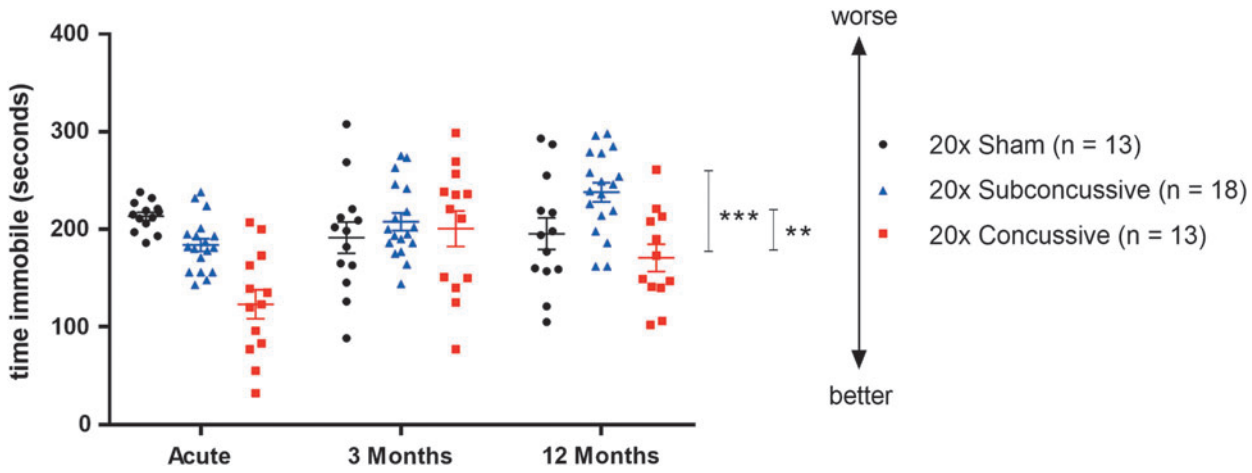

FIG. 8. Effects of injury on depressive-type behavior. The tail suspension test was used to assess depressive-type behavior in animals. There was a significant effect of injury (20×concussive vs. sham: $p = 0.00427$, 20×concussive vs. 20×subconcussive: $p = 0.000212$) with less immobility in the 20×concussive group. Color image is available online.

Downloaded by Washington Univ from www.liebertpub.com at 05/06/19. For personal use only.

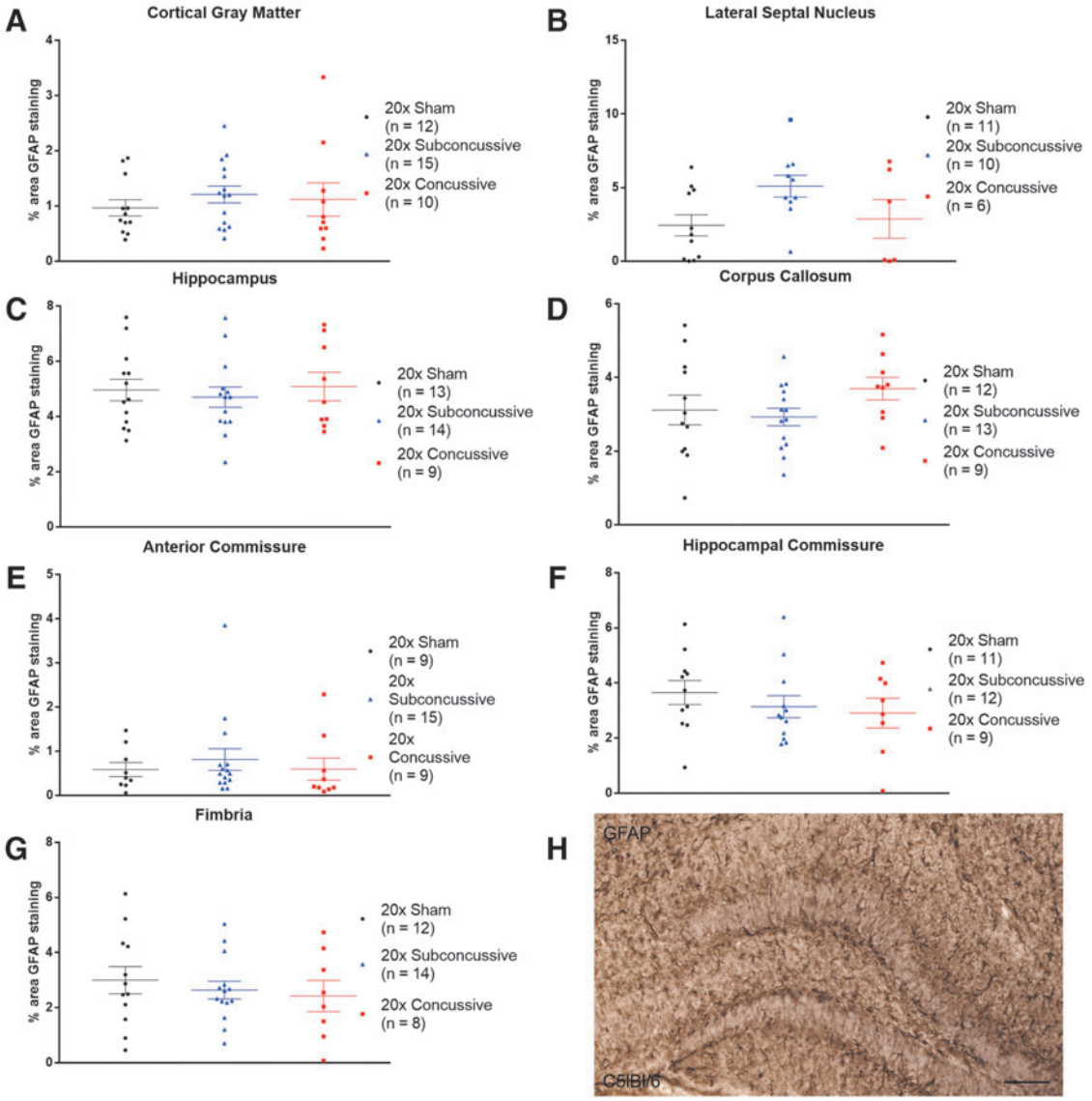

FIG. 9. No effects of injury on chronic astrogliosis. **(A)** Percent area of glial fibrillary acidic protein (GFAP) staining was measured in cortical gray matter. There were no differences in staining between injury groups. **(B)** There was no difference in GFAP staining between injury groups in the lateral septal nucleus. **(C)** No differences in GFAP staining were detected in the hippocampus **(D).** No differences in GFAP staining were detected in the corpus callosum **(E)**. There were no differences between injury groups detected in the anterior commissure. **(F).** No differences in GFAP staining were detected in the hippocampal commissure. **(G).** No differences in GFAP staining were detected in the fimbria. **(H).** GFAP staining in a positive control wild-type mouse injured using controlled cortical impact shows extensive astrogliosis in the hippocampus contralateral to the injury site. Scale bar = 100 microns. Color image is available online.

concussive injury results in white matter microgliosis in the chronic phase of injury.

No evidence of phosphorylated tau pathology in hTau mice

PCR genotyping confirmed that mice from both cohorts were positive for human tau (Supplementary Fig. 11A; see online supplementary material at http://www.liebertpub.com). Total human tau (HT7) was detected using Western blotting for animals from all injury groups and in both cohorts (Supplementary Fig. 11B). A 22-month-old 3xTG mouse was used as a positive control for total and phosphorylated tau. Phosphorylated tau could not be detected in either hTau mice or 3xTG mice using Western blotting for AT8, (Supplementary Fig. 11B), CP13 or AT180. Dot blot analysis with high levels of protein showed that all three antibodies for phosphorylated tau were successfully capable of detecting phosphorylated tau in aged 3xTG but not hTau mice (Supplementary Fig. 11C). Further, hTau mice did not show any substantive staining for HT7, AT8 (ptau, ser202/thr205), CP13 (ptau, ser202) or RZ3 (ptau, thr231; Fig. 11A). However, the aged 3xTG positive control tissue showed extensive positive staining for total tau and phosphorylated tau epitopes (Fig. 11B).

Repetitive injury results in chronic white matter disruption

βAPP staining in hTau animals revealed no abnormalities of axonal profiles at 1 year post-injury, particularly when compared with the axonal swellings clearly visible in the ipsilesional regions of

Downloaded by Washington Univ from www.liebertpub.com at 05/06/19. For personal use only.

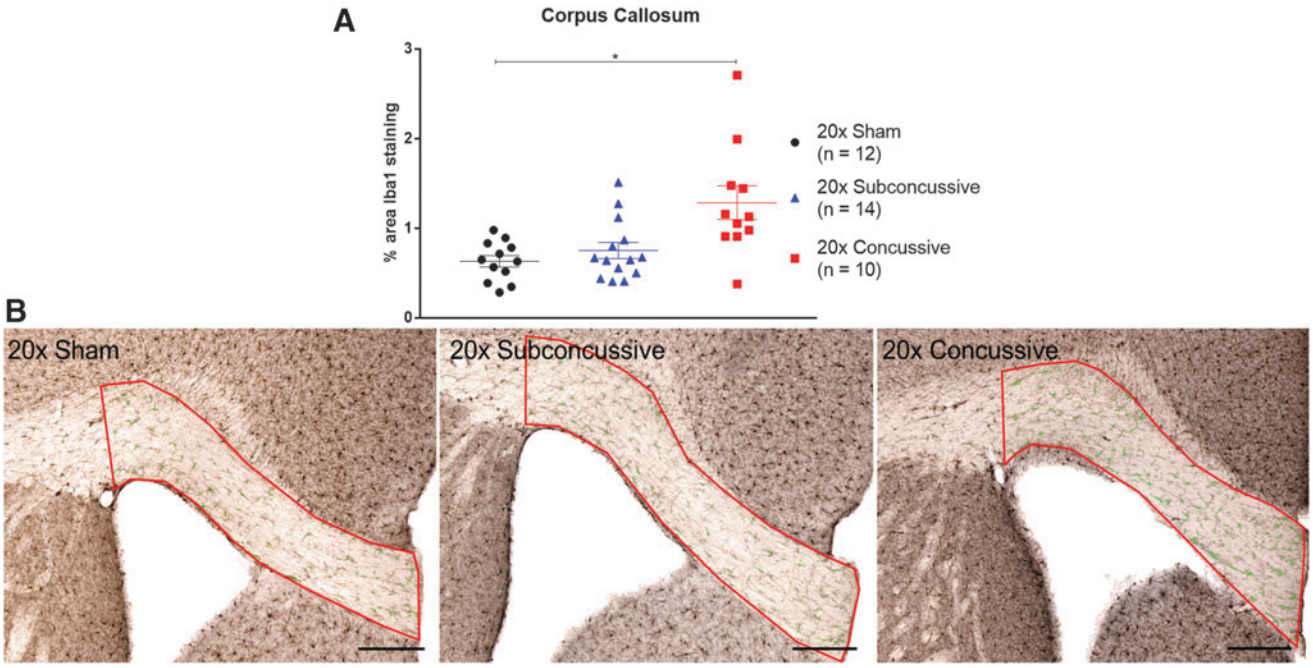

FIG. 10. Repetitive head injuries results in modest increases of activated microglia in the corpus callosum. **(A).** Percent area of thresholded Iba1 staining was significantly increased in animals sustaining 20×concussive injuries at the chronic time-point relative to 20×shams ($p=0.0327$). **(B)** Staining was thresholded using the Sauvola thresholding method in order to quantify Iba1 staining. The automated thresholding method identified increased microglial cell bodies in the 20×concussive animals relative to shams. Scale bar=200 microns. Color image is available online.

animals injured using a controlled cortical impact injury as a positive control (Supplementary Fig. 12; see online supplementary material at http://www.liebertpub.com). We therefore assessed white matter integrity using power coherence as previously described.[33] Power coherence analysis of Myelin Black Gold II stained images was used to measure chronic white matter disruption (Fig. 12). White matter regions of interest included the corpus callosum, anterior commissure, hippocampal commissure and fimbria. The two-way ANOVA showed an effect of injury on power coherence in the corpus callosum [$F(2,37)=28.048$, $\eta^2_p=0.644$, $p<0.00001$], hippocampal commissure [$F(2,37)=34.015$, $\eta^2_p=0.687$, $p<0.00001$] and fimbria [$F(2,37)=17.262$, $\eta^2_p=0.527$, $p<0.00001$] that remained significant following *post hoc* Tukey's testing (Fig. 13). hTau animals in the 20×concussive group had reduced power coherence in the corpus callosum ($p=0.000125$), hippocampal commissure ($p=0.000125$) and fimbria ($p=0.000136$) relative

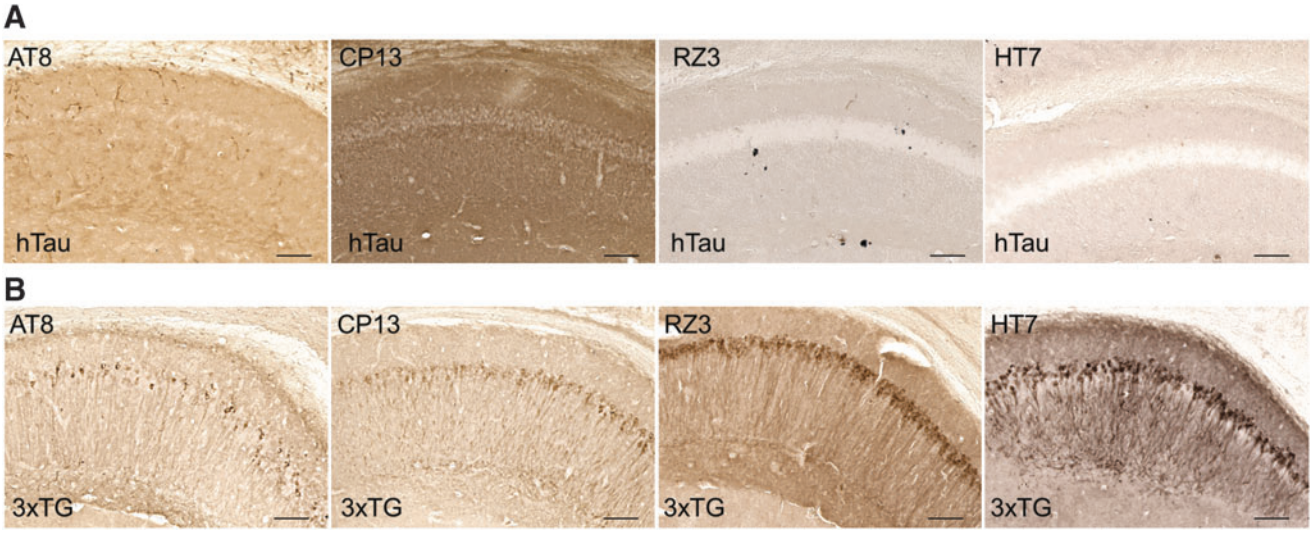

FIG. 11. No detection of tau pathology using immunohistochemistry in any of the hTau mice. **(A)** Monoclonal AT8 (ptau, ser202/thr205), CP13 (ptau, ser202), RZ3 (ptau, Thr231) and HT7 (total tau) were tested to detect phosphorylated and total tau in the hTau mice line. No positive staining was observed for any of the antibodies in any of the groups. **(B)** Tissue from a 22-month-old 3xTG mouse was used as a positive control. When stained with AT8, CP13, RZ3 and HT7 there is extensive positive staining in the hippocampal neurons. Scale bar=100 microns. Color image is available online.

Downloaded by Washington Univ from www.liebertpub.com at 05/06/19. For personal use only.

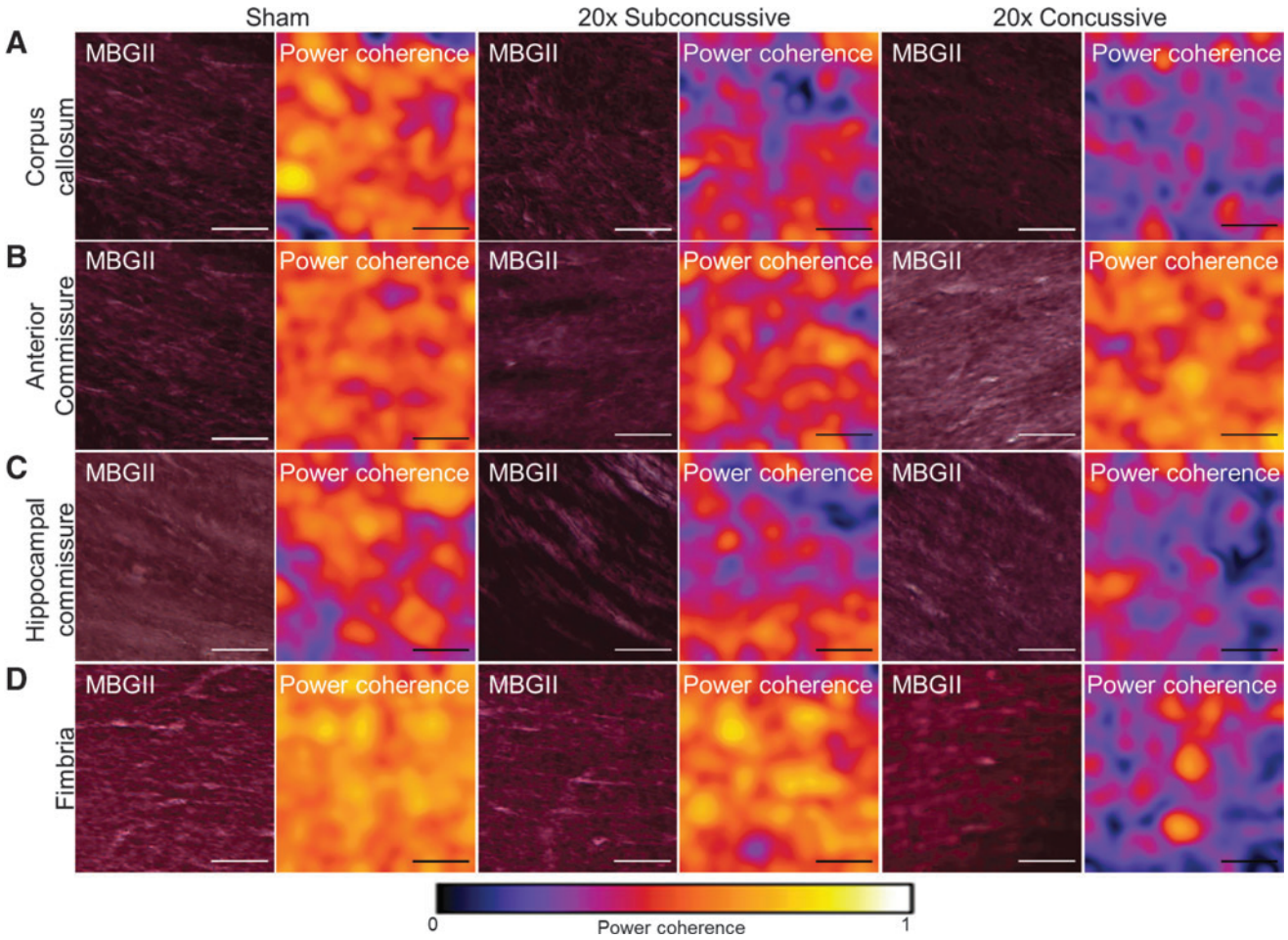

FIG. 12. Effects of injury on chronic white matter disruption, assessed using power coherence. **(A)** Power coherence was measured in the corpus callosum of tissue sections stained with Myelin Black Gold II. Fibers in sham animals have high coherence, indicating that fibers are aligned and intact. However, white matter fibers in injured animals show reduced power coherence, indicating white matter disruption. **(B)** Fibers in the anterior commissure do not show any differences in power coherence, indicating intact white matter. **(C)** Similar to the corpus callosum, white matter in the hippocampal commissure has reduced power coherence, indicating fiber disruption. **(D)** White matter in the fimbria of sham and 20×subconcussive animals shows high power coherence, while the fimbria of 20×concussive animals shows reduced power coherence. Because the fimbria tended to stain more heavily relative to other regions, brightness and contrast levels were uniformly adjusted adjusted for the exemplars so fibers could be better visualized. Scale bars = 50 microns. Color image is available online.

Downloaded by Washington Univ from www.liebertpub.com at 05/06/19. For personal use only.

to shams. Animals in the 20×subconcussive group also showed more modestly reduced power coherence only in the corpus callosum ($p = 0.0091$) and hippocampal commissure ($p = 0.027$) relative to shams. Power coherence was also significantly reduced in the corpus callosum ($p = 0.000367$), hippocampal commissure ($p = 0.000150$), and fimbria ($p = 0.000189$) in the 20×concussive group relative to animals in the 20×subconcussive group.

Because we found evidence of chronic white matter microgliosis following repetitive head injury, we also asked whether there was a relationship between power coherence and microgliosis in white matter tracts (Fig. 14). Interestingly, we found a weak-modest negative correlation between microgliosis and power coherence in the corpus callosum that remained significant after correction for multiple comparisons ($r = -0.441$, $p = 0.0081$). This relationship was weak and insignificant when analyzing the 20×concussive group alone. None of the other white matter tracts showed significant relationships when considering the full sample of animals or injury groups separately. The injury dependent reduction in power coherence suggests that repetitive brain injuries cause acute white matter disruption that remains unresolved in the chronic phase of injury. The difference in effect sizes when comparing coherence in white matter indicates that the corpus callosum and hippocampal commissure may be especially useful regions to assess chronic histological outcomes. Further, white matter disruption in these tracts white matter disruption is concomitant, not correlated with microgliosis.

Correlation between white matter disruption and behavioral performance deficits

To address the question of whether there was a relationship between white matter disruption and the cognitive and motor deficits observed during the Morris water maze task, we performed Spearman's rank correlations between white matter power coherence data collected from the chronic test session of Morris water maze (Fig. 15; Table 1). This was followed by Bonferroni correction for multiple comparisons where the effective number of tests was adjusted by the variance of the eigenvalues of the correlation matrix.[35] We found a

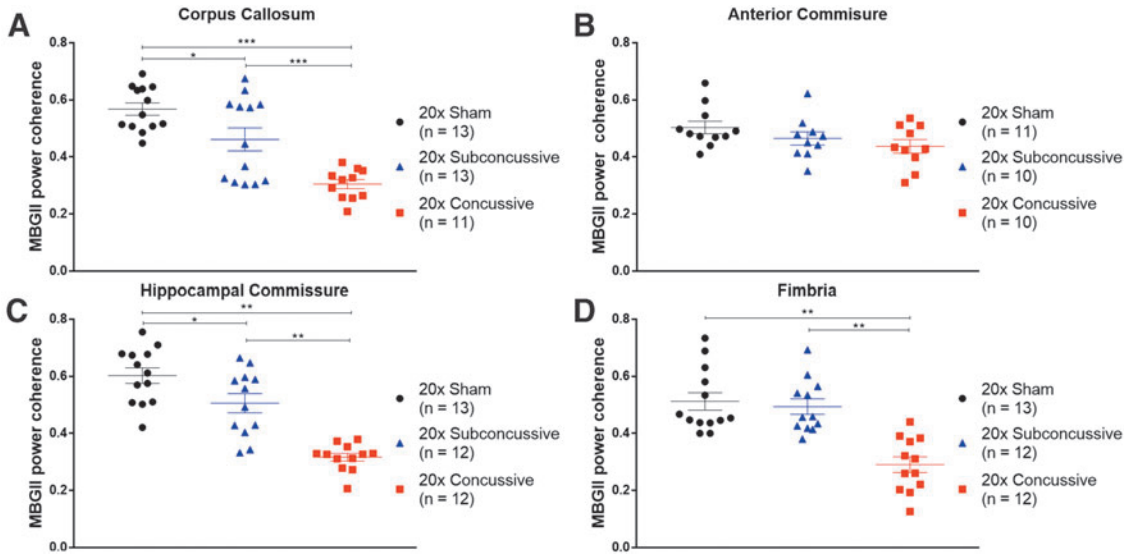

FIG. 13. Reduced white matter integrity following repetitive injury. **(A)** Power coherence in the corpus callosum was significantly reduced in injured animals (20×concussive vs. sham, p=0.000125, 20×subconcussive vs. sham, $p=0.0091$). There was also a significant difference in power coherence between animals in the 20×concussive and 20×subconcussive groups ($p=0.000367$). **(B)** Power coherence in the anterior commissure showed no effect of injury. **(C)** There was a significant effect of injury on power coherence in the hippocampal commissure of hTau animals (20×concussive vs. sham, $p=0.000125$, 20×subconcussive vs. sham, $p=0.027$). There was also a significant difference between animals in the 20×concussive and 20×subconcussive groups ($p=0.000150$). **(D)** Power coherence in the fimbria was significantly reduced in animals in the 20×concussive group (20×concussive vs. sham, $p=0.000136$, 20×concussive vs. 20×subconcussive, $p=0.000189$). Color image is available online.

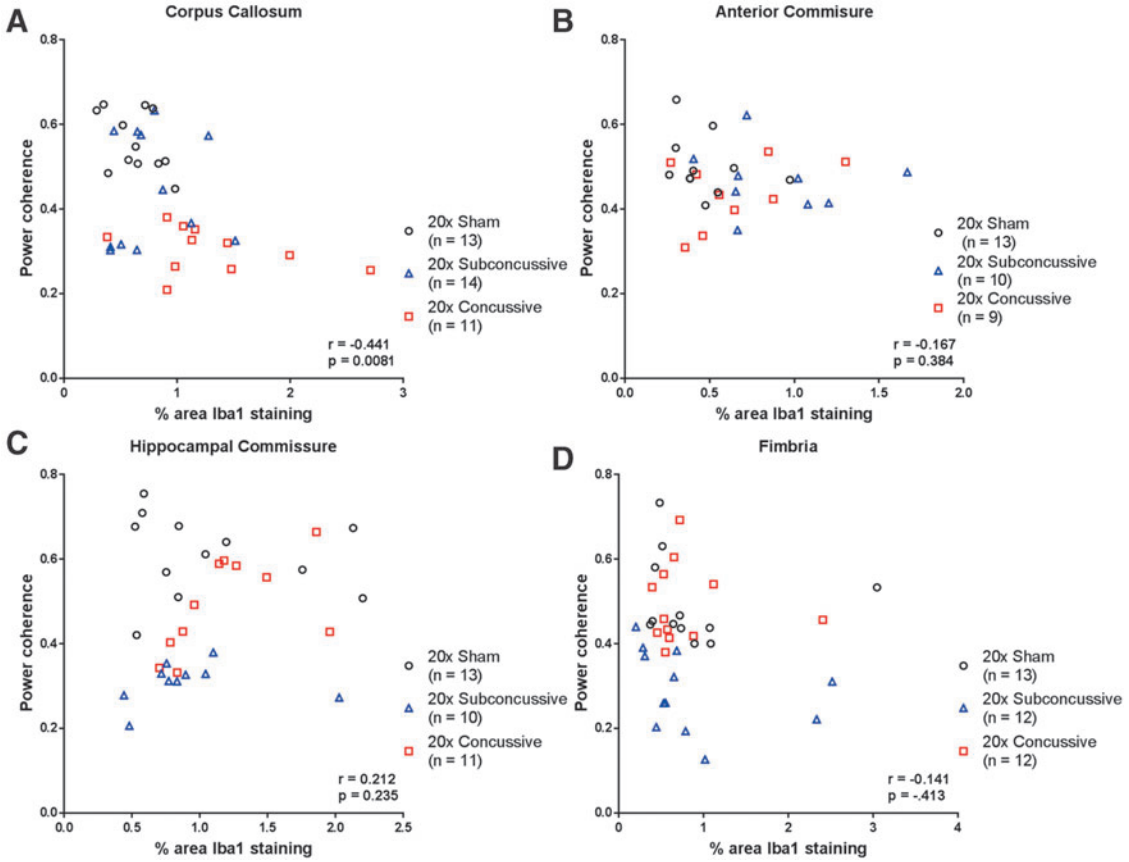

FIG. 14. Relationship between microgliosis and white matter disruption. **(A)** Microgliosis, assessed by percent area of Iba1 staining, showed modest, negative correlation with power coherence in the corpus callosum when considering the full sample of hTau animals. **(B)** In the anterior commissure, microgliosis had a weak and insignificant relationship with power coherence. **(C)** Power coherence in the hippocampal commissure was weakly correlated with microgliosis, a relationship that was not significant after correction for multiple comparisons. **(D)** Spearman's correlation of microgliosis and power coherence in the fimbria showed no significant relationship. Color image is available online.

Downloaded by Washington Univ from www.liebertpub.com at 05/06/19. For personal use only.

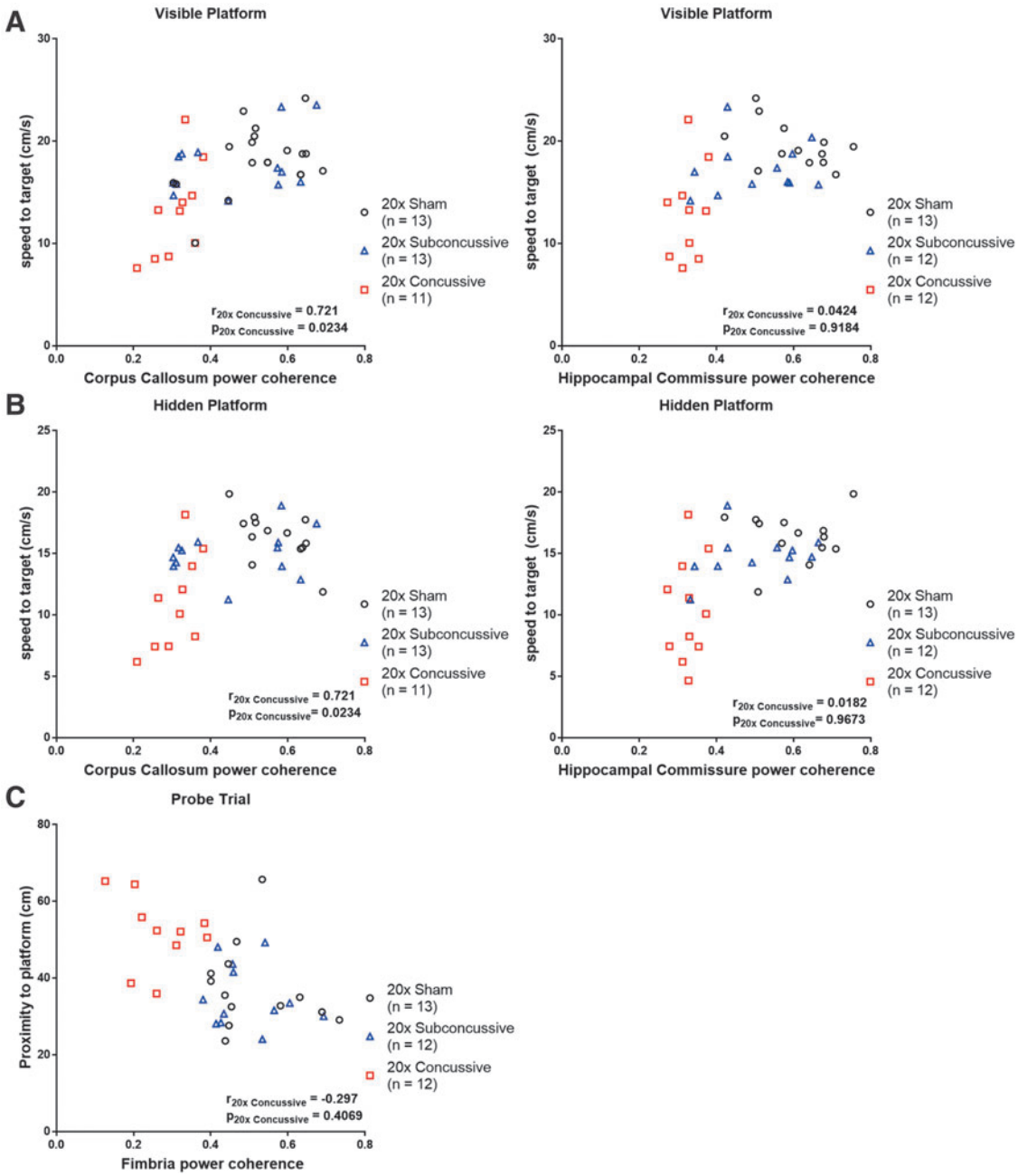

FIG. 15. Relationship between white matter disruption and Morris water maze deficits. **(A)** There was a modest, significant relationship between power coherence in the corpus callosum and swimming speed during the visible platform phase. When considering the 20×concussive group alone, this relationship remained consistent. In the hippocampal commissure, animals in the 20×concussive groups had weak, insignificant correlation of power coherence and swim speed. **(B)** A similar trend was observed in both the corpus callosum and hippocampal commissure during the hidden platform phase. **(C)** Animals that were further away from the platform during probe trial tended to sustain more severe chronic white matter damage in the fimbria. There was a modest but significant relationship between power coherence in this region and proximity to platform. However, in the 20×concussive group, this relationship was weak and no significant relationship between power coherence in the fimbria and proximity to platform during probe trial. Color image is available online.

modest but significant relationship between power coherence in the corpus callosum and swimming speed during both visible and hidden phases. When analyzing the 20×concussive group in isolation, this correlation remained moderate and significant. There also was a moderate correlation between white matter power coherence in the hippocampal commissure and swimming speed during both visible and hidden phases. However, when considering the 20×concussive injury group in isolation, this relationship was weak and not significant. There were no significant correlations between white matter damage and distance to platform measures. Finally, we found a modest but significant relationship between power coherence in the fimbria and proximity to platform during probe trial. This relationship weakened and was not significant when considering the 20×concussive group in isolation.

Downloaded by Washington Univ from www.liebertpub.com at 05/06/19. For personal use only.

Table 1. Correlations of Morris Water Maze Behavior and White Matter Integrity

Behavioral measure	*White matter region*	$p_{full\ sample}$	$r_{full\ sample}$	$p_{20x\ Sham}$	$r_{20x\ Sham}$	$p_{20x\ Subconcussive}$	$r_{20x\ Subconcussive}$	$p_{20x\ Concussive}$	$r_{20x\ Concussive}$
Visible: swim speed	Corpus callosum	**0.000222**	0.578	0.1930	0.312	0.1822	0.396	0.0234	0.721
Hidden: swim speed	Corpus callosum	**0.002689**	0.485	0.1014	–0.478	0.5053	0.203	0.0234	0.721
Visible: swim speed	Hippocampal commissure	**0.00262**	0.493	0.1460	–0.429	0.4169	0.259	0.9184	0.0424
Hidden: swim speed	Hippocampal commissure	**0.000409**	0.558	0.6300	–.1484	0.1474	0.4476	0.9673	0.0182
Probe trial: proximity to platform	Fimbria	**0.00228**	–0.499	0.4477	–0.2308	0.9910	–0.00700	0.4069	–0.297

A Spearman's correlation was used to determine whether there were any significant correlations between white matter power coherence and the cognitive and motor dysfunctions observed during Morris water maze. The p values in bold remained significant after adjusted Bonferroni correction for multiple comparisons ($p < 0.0027$).

We next asked whether there was an association of microgliosis in gray and white matter regions with cognitive deficits observed during the chronic test session of Morris water maze. Spearman's rank analyses showed modest and positive relationships between percent area of Iba1 staining in the corpus callosum, distance to target during the hidden phase, and proximity to platform during probe trial that remained significant after adjusted Bonferroni correction for multiple comparisons (Fig. 16; Table 2). When analyzing the 20×concussive group alone, these relationships weakened and were not significant. The modest correlations for total hTau mice appeared to be driven by animals in the 20×sham group, where the relationships remained moderate but insignificant. Interestingly, we also found that while the relationship between microgliosis in the anterior commissure and distance to target during hidden platform phase was weak and insignificant for the full sample of hTau mice, this correlation was strong and significant

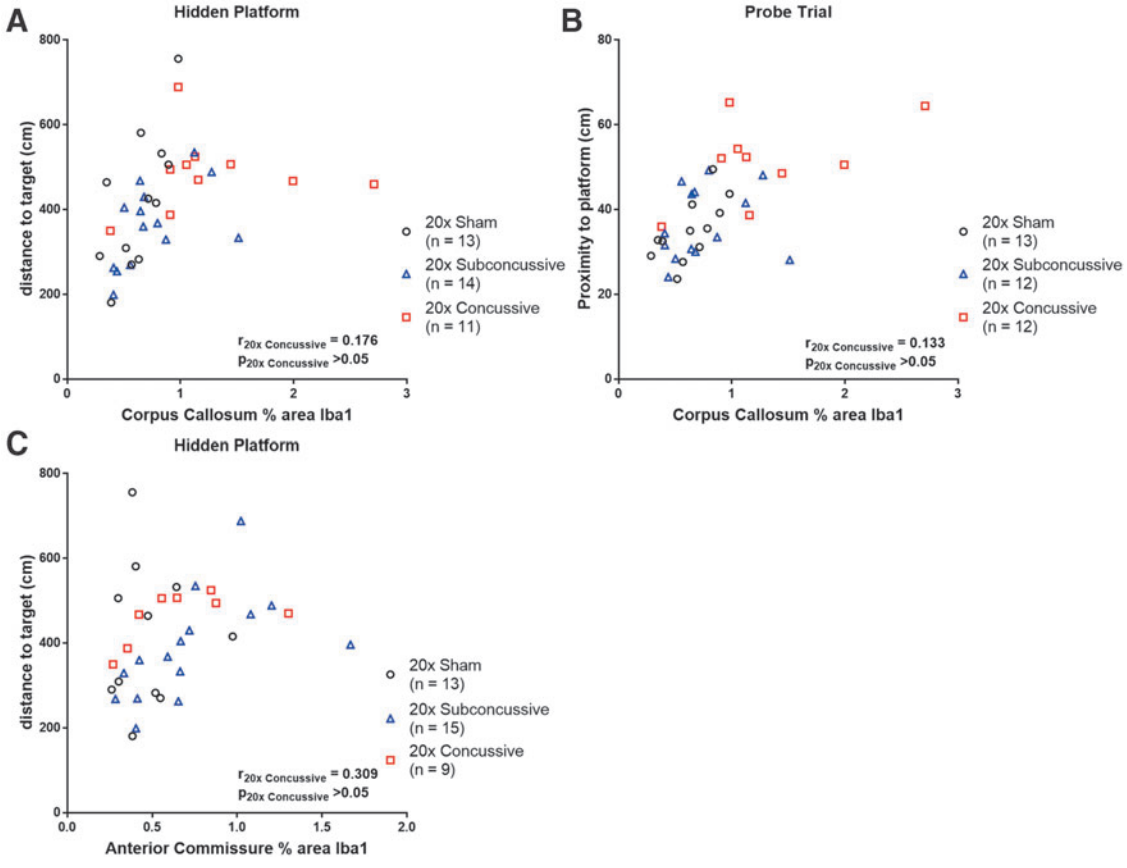

FIG. 16. Relationship between white matter microgliosis and Morris water maze deficits. **(A)** There was a modest, positive relationship between microgliosis in the corpus callosum and distance to target during the hidden platform phase. When considering the 20×concussive group separately, this relationship was weak and not significant. **(B)** Microgliosis in the corpus callosum was also modestly and significantly correlated with proximity to platform during probe trial. In the 20×concussive group, this relationship was weak and insignificant. **(C)** While microgliosis in the anterior commissure did not show a strong relationship with any Morris water maze measures when considering the full sample of hTau animals, analysis of the 20×subconcussive group showed strong and significant correlation of anterior commissure microgliosis and distance to target during hidden platform. Color image is available online.

Downloaded by Washington Univ from www.liebertpub.com at 05/06/19. For personal use only.

Table 2. Correlations of Morris Water Maze Behavior and Microgliosis

Behavioral measure	*Region of interest*	$p_{full\ sample}$	$r_{full\ sample}$	$p_{20x\ Sham}$	$r_{20x\ Sham}$	$p_{20x\ Subconcussive}$	$r_{20x\ Subconcussive}$	$p_{20x\ Concussive}$	$r_{20x\ Concussive}$
Hidden: distance to target	Corpus callosum	**0.000028**	0.639	0.020	0.656	0.030	0.578	0.627	0.176
Hidden: distance to target	Anterior commissure	0.022	0.391	0.894	–0.045	**0.00034**	0.800	0.102	0.309
Probe trial: proximity to platform	Corpus callosum	**0.000089**	0.613	0.0074	0.727	0.418	0.235	0.732	0.133

A Spearman's correlation was used to determine whether there were any significant correlations between microgliosis (% area of Iba1 staining) in gray and white matter regions and the cognitive and motor dysfunctions observed during Morris water maze. The p values in bold remained significant after adjusted Bonferroni correction for multiple comparisons ($p < 0.0015$).

when considering animals in the 20× subconcussive group in isolation. These results indicate that microgliosis and white matter disruption in the corpus callosum, along with damage to tracts such as the hippocampal commissure and fimbria is related to behavioral deficits exhibited during the Morris water maze task.

Discussion

We have implemented a repetitive subconcussive and concussive brain injury paradigm and reported acute, subacute, and chronic behavioral outcomes, as well as histological outcomes at 1 year following injury. We found that repetitive concussive injuries in adult mice result in acute cognitive and motor dysfunction that remains unresolved at up to 1 year post-injury. Further, repetitive concussive injuries caused chronic white matter disruption and microgliosis in several regions of the brain that was moderately correlated with deficits in swimming speed and memory during Morris water maze testing.

Our findings show some consistencies with previous repetitive brain injury models. Multiple repetitive injury models have shown that daily injuries result in cognitive deficits that manifest acutely and persist as late as 6 months to 1 year following injury.[8,9,36] These results show some relevance to the manifestation of behavioral symptoms in patients diagnosed with CTE postmortem. These patients can be classified into two categories: the first group of patients present with mood and behavioral disturbances at an early age (~35 years old) followed by later cognitive deterioration, while the second group presents with cognitive symptoms at an older age (~60 years old) followed by further progression into dementia.[37] The robust findings of persistent cognitive impairment are most clearly relevant to the second group.

When studying other behavioral domains, such as anxiety, social, or depressive behavior, the results become more challenging to reproduce in animal models. For example, mice injured using repetitive injury paradigms do not consistently show deficits when assayed using the open field maze or elevated plus maze, a result paralleled in our work. This could be explained by the sensitivity of these tests to external conditions, such as background noise, lighting conditions and time of day. In particular, tests such as open field maze lack a standardized metric, instead often using distance traveled or time in a user defined periphery zone of the testing box. We attempted to address this deficiency by using time-weighted distance from the maze center as a measure of thigmotaxis, but still found no differences in anxiety related behavior following injury. Our findings in relation to depressive behavior using the tail suspension test proved to be counterintuitive. Although injured animals showed impaired swimming speed during Morris water maze, injured animals had greater mobility times during the tail suspension task, a finding contradicted by previous work using the same behavioral assay.[6,38] The increased mobility may indicate increased hyperactivity following injury. However, sham hTau animals also had surprisingly long immobility times compared with wild-type animals of comparable age.[39] The findings are therefore difficult to interpret without additional data from other tests of depressive behavior such as sucrose preference or the forced swim test, as well as testing tail suspension in the absence of prior stressors such as Morris water maze testing.[40,41]

Interpretation of our histological findings in the context of previous work shows mixed results. Our data show injury related differences in chronic white matter integrity measured using power coherence. Further, there were region specific correlations of white matter disruption and impairments in swimming speed and spatial memory, specifically in the corpus callosum, hippocampal commissure, and fimbria. The large effect sizes in both the corpus callosum and hippocampal commissure indicate that these regions may be useful targets when assessing chronic histological outcomes following therapeutic trials. Previous repetitive injury paradigms have shown reduced white matter volume in the intermediate period following injury[11] but detected no changes in SMI31 immunoreactivity at 6 months post-injury.[36] Moreover, Bennett and colleagues[42] and Shitaka and colleagues[10] both found that APP-positive swellings did not distinguish between sham and injured animals within 1 week following mild repetitive closed-skull traumatic brain injury. Similarly, we found no evidence of abnormalities in axonal profiles that were immunoreactive for βAPP in hTau animals 1 year following repetitive head injuries. These findings indicate that chronic white matter degeneration may not be detectable solely by measuring disruptions in APP transport. We have previously observed reduced white matter integrity measured by power coherence in the regions adjacent to tau laden sulcal depths in ex vivo Stage III/Stage IV CTE human cortical tissue.[43] However, it remains uncertain whether this white matter disruption is a consequence of acute axonal injury, myelin degeneration, or an increased microglial or astrocytic response.

Our findings of correlations of fiber integrity in the corpus callosum and hippocampal commissure with swim speed were surprising and indicate a need for further investigation into the microstructural changes in gray matter in the chronic phase following brain injury, as these may be better predictors of cognitive outcomes such as swimming distance. We attempted to address this question by measuring both microgliosis and astrogliosis gray and white matter regions. Measures of microgliosis assessed by Iba1 immunoreactivity revealed only modest injury related differences in the corpus callosum of animals in the repetitive concussive injury group. Further, microgliosis in the corpus callosum was modestly correlated spatial learning (distance to target, hidden platform) and spatial memory (proximity to platform, probe trial) deficits exhibited during Morris water maze. This finding is paralleled in the work of Mouzon and colleagues, who also found evidence of chronic microgliosis in the corpus callosum accompanied by spatial learning

Downloaded by Washington Univ from www.liebertpub.com at 05/06/19. For personal use only.

deficits in wild-type mice 24 months after repetitive head injuries.[44] Similar to this study, we observed no evidence of injury related microgliosis in any gray matter regions of interest. Interestingly, we found no differences in astrogliosis assessed by GFAP immunoreactivity between sham and injured groups. We used percent area of staining as our metric, which is not sensitive to morphological differences in astrocytes or microglia. Quantification of changes in cell body and process shape would be an alternative method, but would require the use of fluorescent markers and image acquisition at high magnifications for optimal analysis.[45] However, with the growing interest in the relationship between neuroinflammation and ptau in neurodegenerative disease, such experiments may be worth exploring.[46,47] A further area requiring future investigations will be analysis of synapse loss and its relationship with behavioral deficits.[48]

The main strength of this study is that it is one of a few that has followed a population of mice out to 16 months of age and recorded behavioral data from the same mice at acute, intermediate (3-month) and chronic (1-year) time-points post-injury. Importantly, the injury-related deficits in learning and memory we observed are apparent at the chronic time-point, while previous studies have shown cognitive and behavioral deficits acutely that either resolve by the intermediate phase, or do not use a more long-term time-point (9–12 months post-injury) when measuring chronic behavioral outcomes. There also are several strengths when considering the design of the study. First, the use of the transgenic hTau mouse line allowed us to eliminate potential confounds of the differences in tau isoforms between mice and humans. Second, mice were injured at 4 months of age, when phosphorylated tau tangles are not yet present in the hippocampus or cortex. This age at time of injury was selected to better parallel the age at which many patients with CTE sustain repetitive injuries.[3,49] Third, our choice of the non-surgical CHIMERA model allowed for increased number and frequency of injuries that combined both direct impact and rotational acceleration components experienced during a traumatic brain injury.

The negative outcomes of this study reveal several limitations. The first and perhaps most important, is the choice of energy level for repeated concussive and subconcussive impacts. Our LRR data used to inform the selection of 0.13J and 0.24J for subconcussive and concussive injuries showed that animals injured with at least one impact had increased righting times relative to shams. Moreover, we found that animals injured 20 times with 0.24J impacts had increased righting times relative to animals in the 20× subconcussive group and shams, as well as a significantly reduced survival rate in the intermediate and chronic phases following injury. These findings are inconsistent with previous studies using the CHIMERA device, which defined injuries with energy levels below 0.4J as ''subthreshold.''[28] However, these assessments were performed after a maximum of two impacts and did not address the question of cumulative effects of repetitive subthreshold injuries.[28,50]

Previous work in the field of repetitive subthreshold injuries in a rat model has shown that while a single subthreshold impact does not result in pathology, repeated injuries can acutely result in histological abnormalities such as increases in microtubule associated protein, phosphorylated neurofilament, and increased ptau immunoreactivity.[51] In humans, a combination of number of injuries as well as impact velocity shows a threshold-dose response when predicting late-life cognitive dysfunction and mood dysregulation.[52] One possible future direction would be to increase the energy intensities, using 0.4J as the concussive threshold while maintaining the same frequency and number of injuries. This might better address the question of the differences in neurobehavioral and neuropathological trajectory following repetitive subconcussive and concussive injuries.

A second limitation is the use of a lissencephalic animal when attempting to develop an animal model of CTE, where the formation and distribution of ptau pathology is attributed to injury of cortical tissue. In humans, these structures are highly folded, and the curvature of fibers may result in increased vulnerability to mechanical insult and subsequent aggregation of ptau tangles and astroglial tau.[53] Additionally, the composition of the rodent brain, which has a substantially lower white: gray matter ratio relative to humans could also be a reason for the lack of replication of ptau pathology found in CTE.[54] Future studies in animals with gyrencephalic brain architecture, such as ferrets or pigs, would be more relevant when understanding the relationship between repetitive brain injury and chronic histopathological and behavioral deficits found in humans.[25,55–57]

An unexpected limitation of this work is the lack of tau pathology in the hTau mice. Previous studies in the hTau mouse line have shown that uninjured animals are expected to develop neurofibrillary tangles in the hippocampus and cortex starting at 9 months of age, verified using immunohistochemistry, Western blot, and enzyme-linked immunosorbent assay (ELISA) assays.[18,21] Western blotting for total human tau and PCR genotyping confirmed that animals from both cohorts and all injury groups were indeed producing human tau. Surprisingly, Western blotting for tau phosphorylated at different epitopes was not successful in hTau or 3xTG mice. Further, an array of monoclonal antibodies specific for both total tau and ptau showed minimal staining in hTau mice compared with a 22-month-old 3xTG positive control. An additional dot blot assay using these same antibodies confirmed the presence of phosphorylated tau in aged 3xTG animals but not hTau mice. While the positive control would be expected to have increased tau staining because of the triple transgene, this does not explain the lack of positive staining in the hTau line. This could instead be attributed to relatively low abundance of human tau in the hTau tissues, therefore requiring more refined immunohistochemistry steps, such as reduced slice thickness or use of immunofluorescence for more sensitive detection of epitopes.

The issue of low abundance might also explain the negative Western blot results, indicating the need for increased loaded protein during such assays, particularly when studying hTau mice. However, the role of mature neurofibrillary tangles as a driver of neurotoxicity has recently come into question. Tagge and colleagues demonstrated that repeated closed head impacts in wild-type mice resulted in increased cis-ptau histopathology as late as 5 months post-injury, while CP13 levels measured using immunoblot analysis were elevated at 2 weeks post-injury.[58] These findings indicate that there is indeed an upregulation of ptau proteoforms in the months following injury that may precede the formation of tangles. Additionally, recent work has shown that soluble tau oligomers may have increased toxicity relative to fully mature neurofibrillary tangles that potentially have a neuroprotective effect for neurons.[59] Analysis of soluble tau species may therefore provide a better correlate with injury and the cognitive dysfunction that we observed.

The choice of pentobarbital as anesthesia during CSF collection and tissue extraction is also a potential confound of this study. The reduction in respiratory rate during this mode of anesthesia could result in unexpected histopathological effects, such as an altered inflammatory or astrocytic response.[45,60] While we did not see any differences in astrocytosis as evidenced by GFAP staining in any region, an acute astroglial response following pentobarbital injection would explain the levels of astrocytes observed in the gray and white matter regions of both injured and sham hTau mice. This

Downloaded by Washington Univ from www.liebertpub.com at 05/06/19. For personal use only.

would be best addressed by performing GFAP staining in animals perfused using an alternative method of anesthesia, such as isoflurane, on littermates.

Additional future directions of this study include analysis of the CSF and blood samples for tau, GFAP, and other brain proteins. These will allow us to explore the question of whether repetitive brain injury results in changes of soluble tau species or impairs long-term blood brain barrier integrity. Further, ELISAs and other assays of the fresh-frozen tissue samples collected from the hTau mice will provide an alternative to histopathology to determine whether there is evidence of phosphorylated tau in the brain.

In summary, a repetitive CHIMERA injury paradigm implemented in adult mice results in persistent behavioral dysfunction that is linked to disruption of specific white matter tracts. This disruption, detected by calculation of power coherence from myelin staining, shows that white matter damage occurs in a graded manner based on the intensity of repeated impacts, coinciding with behavioral deficits. These outcomes show that impacts previously considered ''subthreshold'' do result in lasting tissue damage in the brain.

Downloaded by Washington Univ from www.liebertpub.com at 05/06/19. For personal use only.

Acknowledgments

The authors thank Theodore Floros for his contribution when measuring righting times following injuries, as well as the remaining members of the Brody laboratory for helpful discussion of the data presented here. We would also like to thank Terrance Kummer, MD, PhD, and Andrew Sauerbeck, PhD, for development of open field thigmotaxis that was used as one of our outcome measures, and Kathleen Schoch, PhD, for providing hTau tail DNA used as the positive control during PCR. Finally, we are grateful to Hao Jiang, PhD, for extensive effort and helpful discussion when performing Western blot experiments. Acquisition of histological images was performed in part through the use of Washington University Center for Cellular Imaging (WUCCI) supported by Washington University School of Medicine, The Children's Discovery Institute of Washington University and St. Louis Children's Hospital (CDI-CORE-2015-505) and the National Institute of Neurological Disorders and Stroke (NS086741). This work was supported by DMRDP PT110816 and NIH R01 NS065069 (PI: Brody) and the Center for Neuroscience and Regenerative Medicine. The views expressed here are those of the authors.

Author Disclosure Statement

No competing financial interests exist.

References

1. Bieniek, K.F., Ross, O.A., Cormier, K.A., Walton, R.L., Soto-Ortolaza, A., Johnston, A.E., DeSaro, P., Boylan, K.B., Graff-Radford, N.R., Wszolek, Z.K., Rademakers, R., Boeve, B.F., McKee, A.C., and Dickson, D.W. (2015). Chronic traumatic encephalopathy pathology in a neurodegenerative disorders brain bank. Acta Neuropathol. 130, 877–889.
2. Mahar, I., Alosco, M.L., and McKee, A.C. (2017). Psychiatric phenotypes in chronic traumatic encephalopathy. Neurosci. Biobehav. Rev. 83.
3. Mez, J., Daneshvar, D.H., Kiernan, P.T., Abdolmohammadi, B., Alvarez, V.E., Huber, B.R., Alosco, M.L., Solomon, T.M., Nowinski, C.J., McHale, L., Cormier, K.A., Kubilus, C.A., Martin, B.M., Murphy, L., Baugh, C.M., Montenigro, P.H., Chaisson, C.E., Tripodis, Y., Kowall, N.W., Weuve, J., McClean, M.D., Cantu, R.C., Goldstein, L.E., Katz, D.I., Stern, R.A., Stein, T.D., and McKee, A.C. (2017). Clinicopathological evaluation of chronic traumatic encephalopathy in players of American football. JAMA 318, 360–370.
4. McKee, A.C., Cairns, N.J., Dickson, D.W., Folkerth, R.D., Keene, C.D., Litvan, I., Perl, D.P., Stein, T.D., Vonsattel, J.P., Stewart, W., Tripodis, Y., Crary, J.F., Bieniek, K.F., Dams-O'Connor, K., Alvarez, V.E., and Gordon, W.A. (2016). The first NINDS/NIBIB consensus meeting to define neuropathological criteria for the diagnosis of chronic traumatic encephalopathy. Acta Neuropathol. 131, 75–86.
5. McKee, A.C., Stein, T.D., Kiernan, P.T., and Alvarez, V.E. (2015). The neuropathology of chronic traumatic encephalopathy. Brain Pathol. 25, 350–364.
6. Bajwa, N.M., Halavi, S., Hamer, M., Semple, B.D., Noble-Haeusslein, L.J., Baghchechi, M., Hiroto, A., Hartman, R.E., and Obenaus, A. (2016). Mild concussion, but not moderate traumatic brain injury, is associated with long-term depression-like phenotype in mice. PLoS One 11, e0146886.
7. Petraglia, A.L., Plog, B.A., Dayawansa, S., Dashnaw, M.L., Czerniecka, K., Walker, C.T., Chen, M., Hyrien, O., Iliff, J.J., Deane, R., Huang, J.H., and Nedergaard, M. (2014). The pathophysiology underlying repetitive mild traumatic brain injury in a novel mouse model of chronic traumatic encephalopathy. Surg. Neurol. Int. 5, 184.
8. Petraglia, A.L., Plog, B.A., Dayawansa, S., Chen, M., Dashnaw, M.L., Czerniecka, K., Walker, C.T., Viterise, T., Hyrien, O., Iliff, J.J., Deane, R., Nedergaard, M., and Huang, J.H. (2014). The spectrum of neurobehavioral sequelae after repetitive mild traumatic brain injury: a novel mouse model of chronic traumatic encephalopathy. J. Neurotrauma 31, 1211–1224.
9. Luo, J., Nguyen, A., Villeda, S., Zhang, H., Ding, Z., Lindsey, D., Bieri, G., Castellano, J.M., Beaupre, G.S., and Wyss-Coray, T. (2014). Long-term cognitive impairments and pathological alterations in a mouse model of repetitive mild traumatic brain injury. Front. Neurol. 5, 12.
10. Shitaka, Y., Tran, H.T., Bennett, R.E., Sanchez, L., Levy, M.A., Dikranian, K., and Brody, D.L. (2011). Repetitive closed-skull traumatic brain injury in mice causes persistent multifocal axonal injury and microglial reactivity. J. Neuropathol. Exp. Neurol. 70, 551–567.
11. Mannix, R., Berkner, J., Mei, Z., Alcon, S., Hashim, J., Robinson, S., Jantzie, L., Meehan, W.P. 3rd, and Qiu, J. (2017). Adolescent mice demonstrate a distinct pattern of injury after repetitive mild traumatic brain injury. J. Neurotrauma 34, 495–504.
12. Yoshiyama, Y., Uryu, K., Higuchi, M., Longhi, L., Hoover, R., Fujimoto, S., McIntosh, T., Lee, V.M., and Trojanowski, J.Q. (2005). Enhanced neurofibrillary tangle formation, cerebral atrophy, and cognitive deficits induced by repetitive mild brain injury in a transgenic tauopathy mouse model. J. Neurotrauma 22, 1134–1141.
13. Yu, F., Shukla, D.K., Armstrong, R.C., Marion, C.M., Radomski, K.L., Selwyn, R.G., and Dardzinski, B.J. (2017). Repetitive model of mild traumatic brain injury produces cortical abnormalities detectable by magnetic resonance diffusion imaging, histopathology, and behavior. J. Neurotrauma 34, 1364–1381.
14. Mouzon, B.C., Bachmeier, C., Ferro, A., Ojo, J.O., Crynen, G., Acker, C.M., Davies, P., Mullan, M., Stewart, W., and Crawford, F. (2014). Chronic neuropathological and neurobehavioral changes in a repetitive mild traumatic brain injury model. Ann. Neurol. 75, 241–254.
15. Yang, Z., Wang, P., Morgan, D., Lin, D., Pan, J., Lin, F., Strang, K.H., Selig, T.M., Perez, P.D., Febo, M., Chang, B., Rubenstein, R., and Wang, K.K. (2015). Temporal MRI characterization, neurobiochemical and neurobehavioral changes in a mouse repetitive concussive head injury model. Sci. Rep. 5, 11178.
16. Tran, H.T., Sanchez, L., Esparza, T.J., and Brody, D.L. (2011). Distinct temporal and anatomical distributions of amyloid-beta and tau abnormalities following controlled cortical impact in transgenic mice. PLoS One 6, e25475.
17. Tran, H.T. (2011). The association between traumatic brain injury and Alzheimer's disease: mouse models and potential mechanisms [graduate dissertation]. Washington University in St. Louis, St. Louis, Missouri.
18. Andorfer, C., Kress, Y., Espinoza, M., de Silva, R., Tucker, K.L., Barde, Y.A., Duff, K., and Davies, P. (2003). Hyperphosphorylation and aggregation of tau in mice expressing normal human tau isoforms. J. Neurochem. 86, 582–590.
19. Goedert, M., Spillantini, M.G., Jakes, R., Rutherford, D., and Crowther, R.A. (1989). Multiple isoforms of human microtubule-associated protein tau: sequences and localization in neurofibrillary tangles of Alzheimer's disease. Neuron 3, 519–526.
20. Guo, J.L., Narasimhan, S., Changolkar, L., He, Z., Stieber, A., Zhang, B., Gathagan, R.J., Iba, M., McBride, J.D., Trojanowski, J.Q., and

Lee, V.M. (2016). Unique pathological tau conformers from Alzheimer's brains transmit tau pathology in nontransgenic mice. J. Exp. Med. 213, 2635–2654.
21. Polydoro, M., Acker, C.M., Duff, K., Castillo, P.E., and Davies, P. (2009). Age-dependent impairment of cognitive and synaptic function in the htau mouse model of tau pathology. J. Neurosci. 29, 10741–10749.
22. Ojo, J.O., Mouzon, B., Greenberg, M.B., Bachmeier, C., Mullan, M., and Crawford, F. (2013). Repetitive mild traumatic brain injury augments tau pathology and glial activation in aged hTau mice. J. Neuropathol. Exp. Neurol. 72, 137–151.
23. Ojo, J.O., Mouzon, B., Algamal, M., Leary, P., Lynch, C., Abdullah, L., Evans, J., Mullan, M., Bachmeier, C., Stewart, W., and Crawford, F. (2016). Chronic repetitive mild traumatic brain injury results in reduced cerebral blood flow, axonal injury, gliosis, and increased T-tau and tau oligomers. J. Neuropathol. Exp. Neurol. 75, 636–655.
24. Zhang, J., Yoganandan, N., Pintar, F.A., and Gennarelli, T.A. (2006). Role of translational and rotational accelerations on brain strain in lateral head impact. Biomed. Sci. Instrum. 42, 501–506.
25. Smith, D.H., Chen, X.H., Nonaka, M., Trojanowski, J.Q., Lee, V.M., Saatman, K.E., Leoni, M.J., Xu, B.N., Wolf, J.A., and Meaney, D.F. (1999). Accumulation of amyloid beta and tau and the formation of neurofilament inclusions following diffuse brain injury in the pig. J. Neuropathol. Exp. Neurol. 58, 982–992.
26. Namjoshi, D.R., Cheng, W.H., McInnes, K.A., Martens, K.M., Carr, M., Wilkinson, A., Fan, J., Robert, J., Hayat, A., Cripton, P.A., and Wellington, C.L. (2014). Merging pathology with biomechanics using CHIMERA (Closed-Head Impact Model of Engineered Rotational Acceleration): a novel, surgery-free model of traumatic brain injury. Mol. Neurodegener. 9, 55.
27. Chen, H., Desai, A., and Kim, H.Y. (2017). Repetitive closed-head impact model of engineered rotational acceleration induces long-term cognitive impairments with persistent astrogliosis and microgliosis in mce. J. Neurotrauma 34, 2291–2302.
28. Namjoshi, D.R., Cheng, W.H., Bashir, A., Wilkinson, A., Stukas, S., Martens, K.M., Whyte, T., Abebe, Z.A., McInnes, K.A., Cripton, P.A., and Wellington, C.L. (2017). Defining the biomechanical and biological threshold of murine mild traumatic brain injury using CHIMERA (Closed Head Impact Model of Engineered Rotational Acceleration). Exp. Neurol. 292, 80–91.
29. Nadler, J.J., Moy, S.S., Dold, G., Trang, D., Simmons, N., Perez, A., Young, N.B., Barbaro, R.P., Piven, J., Magnuson, T.R., and Crawley, J.N. (2004). Automated apparatus for quantitation of social approach behaviors in mice. Genes Brain Behav. 3, 303–314.
30. DeMattos, R.B., Bales, K.R., Parsadanian, M., O'Dell, M.A., Foss, E.M., Paul, S.M., and Holtzman, D.M. (2002). Plaque-associated disruption of CSF and plasma amyloid-beta (Abeta) equilibrium in a mouse model of Alzheimer's disease. J. Neurochem. 81, 229–236.
31. Oddo, S., Caccamo, A., Shepherd, J.D., Murphy, M.P., Golde, T.E., Kayed, R., Metherate, R., Mattson, M.P., Akbari, Y., and LaFerla, F.M. (2003). Triple-transgenic model of Alzheimer's disease with plaques and tangles: intracellular Abeta and synaptic dysfunction. Neuron 39, 409–421.
32. Mac Donald, C.L., Dikranian, K., Bayly, P., Holtzman, D., and Brody, D. (2007). Diffusion tensor imaging reliably detects experimental traumatic axonal injury and indicates approximate time of injury. J. Neurosci. 27, 11869–11876.
33. Gangolli, M., Holleran, L., Hee Kim, J., Stein, T.D., Alvarez, V., McKee, A.C., and Brody, D.L. (2017). Quantitative validation of a nonlinear histology-MRI coregistration method using generalized Q-sampling imaging in complex human cortical white matter. Neuroimage 153, 152–167.
34. Tran, H.T., LaFerla, F.M., Holtzman, D.M., and Brody, D.L. (2011). Controlled cortical impact traumatic brain injury in 3xTg-AD mice causes acute intra-axonal amyloid-beta accumulation and independently accelerates the development of tau abnormalities. J. Neurosci. 31, 9513–9525.
35. Cheverud, J.M. (2001). A simple correction for multiple comparisons in interval mapping genome scans. Heredity (Edinb.) 87, 52–58.
36. Mannix, R., Meehan, W.P., Mandeville, J., Grant, P.E., Gray, T., Berglass, J., Zhang, J., Bryant, J., Rezaie, S., Chung, J.Y., Peters, N.V., Lee, C., Tien, L.W., Kaplan, D.L., Feany, M., and Whalen, M. (2013). Clinical correlates in an experimental model of repetitive mild brain injury. Ann. Neurol. 74, 65–75.
37. Stern, R.A., Daneshvar, D.H., Baugh, C.M., Seichepine, D.R., Montenigro, P.H., Riley, D.O., Fritts, N.G., Stamm, J.M., Robbins, C.A., McHale, L., Simkin, I., Stein, T.D., Alvarez, V.E., Goldstein, L.E., Budson, A.E., Kowall, N.W., Nowinski, C.J., Cantu, R.C., and McKee, A.C. (2013). Clinical presentation of chronic traumatic encephalopathy. Neurology 81, 1122–1129.
38. Klemenhagen, K.C., O'Brien, S.P., and Brody, D.L. (2013). Repetitive concussive traumatic brain injury interacts with post-injury foot shock stress to worsen social and depression-like behavior in mice. PLoS One 8, e74510.
39. Shoji, H., Takao, K., Hattori, S., and Miyakawa, T. (2016). Age-related changes in behavior in C57BL/6J mice from young adulthood to middle age. Mol. Brain 9, 11.
40. Castagne, V., Moser, P., Roux, S., and Porsolt, R.D. (2011). Rodent models of depression: forced swim and tail suspension behavioral despair tests in rats and mice. Curr. Protoc. Neurosci. Chapter 8, Unit 8 10A.
41. Strekalova, T., Spanagel, R., Bartsch, D., Henn, F.A., and Gass, P. (2004). Stress-induced anhedonia in mice is associated with deficits in forced swimming and exploration. Neuropsychopharmacology 29, 2007–2017.
42. Bennett, R.E., Mac Donald, C.L., and Brody, D.L. (2012). Diffusion tensor imaging detects axonal injury in a mouse model of repetitive closed-skull traumatic brain injury. Neurosci. Lett. 513, 160–165.
43. Holleran, L., Kim, J.H., Gangolli, M., Stein, T., Alvarez, V., McKee, A., and Brody, D.L. (2017). Axonal disruption in white matter underlying cortical sulcus tau pathology in chronic traumatic encephalopathy. Acta Neuropathol. 133, 367–380.
44. Mouzon, B.C., Bachmeier, C., Ojo, J.O., Acker, C.M., Ferguson, S., Paris, D., Ait-Ghezala, G., Crynen, G., Davies, P., Mullan, M., Stewart, W., and Crawford, F. (2018). Lifelong behavioral and neuropathological consequences of repetitive mild traumatic brain injury. Ann. Clin. Transl. Neurol. 5, 64–80.
45. Soltys, Z., Janeczko, K., Orzylowska-Sliwinska, O., Zaremba, M., Januszewski, S., and Oderfeld-Nowak, B. (2003). Morphological transformations of cells immunopositive for GFAP, TrkA or p75 in the CA1 hippocampal area following transient global ischemia in the rat. A quantitative study. Brain Res. 987, 186–193.
46. Kovacs, G.G., Lee, V.M., and Trojanowski, J.Q. (2017). Protein astrogliopathies in human neurodegenerative diseases and aging. Brain Pathol. 27, 675–690.
47. Cherry, J.D., Tripodis, Y., Alvarez, V.E., Huber, B., Kiernan, P.T., Daneshvar, D.H., Mez, J., Montenigro, P.H., Solomon, T.M., Alosco, M.L., Stern, R.A., McKee, A.C., and Stein, T.D. (2016). Microglial neuroinflammation contributes to tau accumulation in chronic traumatic encephalopathy. Acta Neuropathol. Commun. 4, 112.
48. Winston, C.N., Noel, A., Neustadtl, A., Parsadanian, M., Barton, D.J., Chellappa, D., Wilkins, T.E., Alikhani, A.D., Zapple, D.N., Villapol, S., Planel, E., and Burns, M.P. (2016). Dendritic spine loss and chronic white matter inflammation in a mouse model of highly repetitive head trauma. Am. J. Pathol. 186, 552–567.
49. McKee, A.C., Cantu, R.C., Nowinski, C.J., Hedley-Whyte, E.T., Gavett, B.E., Budson, A.E., Santini, V.E., Lee, H.S., Kubilus, C.A., and Stern, R.A. (2009). Chronic traumatic encephalopathy in athletes: progressive tauopathy after repetitive head injury. J. Neuropathol. Exp. Neurol. 68, 709–735.
50. Namjoshi, D.R., Cheng, W.H., Carr, M., Martens, K.M., Zareyan, S., Wilkinson, A., McInnes, K.A., Cripton, P.A., and Wellington, C.L. (2016). Chronic exposure to androgenic-anabolic steroids exacerbates axonal injury and microgliosis in the CHIMERA mouse model of repetitive concussion. PLoS One 11, e0146540.
51. Kanayama, G., Takeda, M., Niigawa, H., Ikura, Y., Tamii, H., Taniguchi, N., Kudo, T., Miyamae, Y., Morihara, T., and Nishimura, T. (1996). The effects of repetitive mild brain injury on cytoskeletal protein and behavior. Methods Find. Exp. Clin. Pharmacol. 18, 105–115.
52. Montenigro, P.H., Alosco, M.L., Martin, B.M., Daneshvar, D.H., Mez, J., Chaisson, C.E., Nowinski, C.J., Au, R., McKee, A.C., Cantu, R.C., McClean, M.D., Stern, R.A., and Tripodis, Y. (2017). Cumulative head impact exposure predicts later-life depression, apathy, executive dysfunction, and cognitive impairment in former high school and college football players. J. Neurotrauma 34, 328–340.
53. Ghajari, M., Hellyer, P.J., and Sharp, D.J. (2017). Computational modelling of traumatic brain injury predicts the location of chronic traumatic encephalopathy pathology. Brain 140, 333–343.

Downloaded by Washington Univ from www.liebertpub.com at 05/06/19. For personal use only.

54. Zhang, K. and Sejnowski, T.J. (2000). A universal scaling law between gray matter and white matter of cerebral cortex. Proc. Natl. Acad. Sci. U. S. A. 97, 5621–5626.
55. Barnette, A.R., Neil, J.J., Kroenke, C.D., Griffith, J.L., Epstein, A.A., Bayly, P.V., Knutsen, A.K., and Inder, T.E. (2009). Characterization of brain development in the ferret via MRI. Pediatr. Res. 66, 80–84.
56. Schwerin, S.C., Hutchinson, E.B., Radomski, K.L., Ngalula, K.P., Pierpaoli, C.M., and Juliano, S.L. (2017). Establishing the ferret as a gyrencephalic animal model of traumatic brain injury: optimization of controlled cortical impact procedures. J. Neurosci. Methods 285, 82–96.
57. Hutchinson, E.B., Schwerin, S.C., Radomski, K.L., Irfanoglu, M.O., Juliano, S.L., and Pierpaoli, C.M. (2016). Quantitative MRI and DTI abnormalities during the acute period following CCI in the ferret. Shock 46, 167–176.
58. Tagge, C.A., Fisher, A.M., Minaeva, O.V., Gaudreau-Balderrama, A., Moncaster, J.A., Zhang, X.L., Wojnarowicz, M.W., Casey, N., Lu, H., Kokiko-Cochran, O.N., Saman, S., Ericsson, M., Onos, K.D., Veksler, R., Senatorov, V.V., Jr., Kondo, A., Zhou, X.Z., Miry, O., Vose, L.R., Gopaul, K.R., Upreti, C., Nowinski, C.J., Cantu, R.C., Alvarez, V.E., Hildebrandt, A.M., Franz, E.S., Konrad, J., Hamilton, J.A., Hua, N., Tripodis, Y., Anderson, A.T., Howell, G.R., Kaufer, D., Hall, G.F., Lu, K.P., Ransohoff, R.M., Cleveland, R.O., Kowall, N.W., Stein, T.D., Lamb, B.T., Huber, B.R., Moss, W.C., Friedman, A., Stanton, P.K., McKee, A.C., and Goldstein, L.E. (2018). Concussion, microvascular injury, and early tauopathy in young athletes after impact head injury and an impact concussion mouse model. Brain 141, 422–458.
59. d'Orange, M., Auregan, G., Cheramy, D., Gaudin-Guerif, M., Lieger, S., Guillermier, M., Stimmer, L., Josephine, C., Herard, A.S., Gaillard, M.C., Petit, F., Kiessling, M.C., Schmitz, C., Colin, M., Buee, L., Panayi, F., Diguet, E., Brouillet, E., Hantraye, P., Bemelmans, A.P., and Cambon, K. (2018). Potentiating tangle formation reduces acute toxicity of soluble tau species in the rat. Brain 141, 535–549.
60. DeWalt, G.J., Mahajan, B., Foster, A.R., Thompson, L.D.E., Marttini, A.A., Schmidt, E.V., Mansuri, S., D'Souza, D., Patel, S.B., Tenenbaum, M., Brandao-Viruet, K.I., Thompson, D., Duong, B., Smith, D.H., Blute, T.A., and Eldred, W.D. (2017). Region-specific alterations in astrocyte and microglia morphology following exposure to blasts in the mouse hippocampus. Neurosci. Lett. 664, 160–166.

Address correspondence to:
David L. Brody, MD, PhD
Washington University School of Medicine
Hope Center for Neurological Disorders
Uniformed Services University of the Health Science
St. Louis, MO 20814-4799

E-mail: brodyd@wustl.edu;
david.brody@usuhs.edu

Downloaded by Washington Univ from www.liebertpub.com at 05/06/19. For personal use only.